Stereoelectronic Effects in Biomolecules
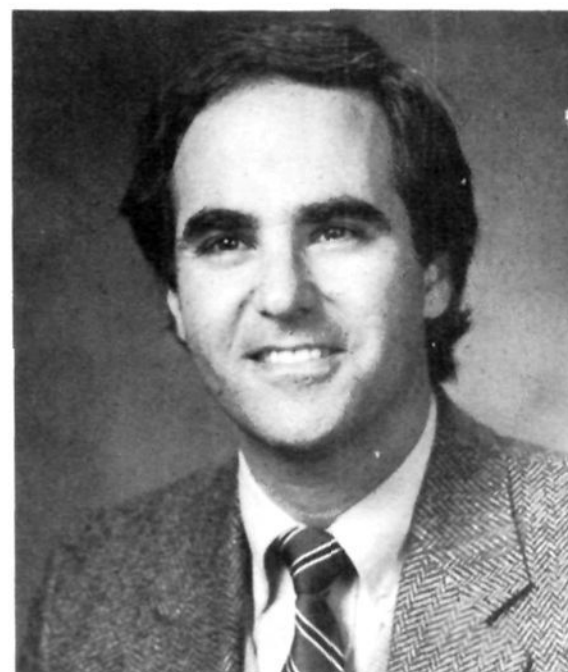
DAVID G. GORENSTEIN

Department of Chemistry, Purdue University, West Lafayette, Indiana 47907

Contents

David Gorenstein is Professor of Chemistry at Purdue University and Director of the Purdue Biochemical Magnetic Resonance Laboratory, a National NMR laboratory supported by Research Resources, NIH, and Biological Instrumentation, NSF. He was born in Chicago and educated in the Boston area, with a 1966 B.S. degree from M.I.T. and a Ph.D. with Frank Westheimer at Harvard in 1969. He then directly joined the University of Illinois at Chicago where he stayed except for a 1-year Senior Fulbright Fellowship at Oxford University in England. In 1985 he moved to Purdue University, West Lafayette, IN, and recently completed a Guggenheim Fellowship at University of California, San Francisco. His research interests include NMR spectroscopy of biological macromolecules, biological reaction mechanisms and enzymology, and bioorganic and theoretical organic chemistry, particularly of phosphorus compounds. More recently he has become involved in protein design and recombinant DNA methodology.

I. Introduction

There has been a growing recognition that conformationally dependent orbital interactions can play a significant role in the structure and reactivity of biomolecules. The stereoelectronic theory of Deslongchamps[1,2] has received support experimentally[1-3] and theoretically,[6-14] and several applications of the theory to enzymatic reactions have also appeared.[2-5,13,14] The theory is not without its critics,[15,16] and it would seem appropriate at this stage of the development of the theory to critically analyze basic concepts and biological applications.

Deslongchamps and co-workers[1,2] in studying tetracovalent carbon species have demonstrated selective cleavage of bonds that are antiperiplanar (app) to lone

pairs on directly bonded oxygen and nitrogen atoms. Thus, as shown in reaction 1, addition of alkoxide to

X = OR″, NR″$_2$
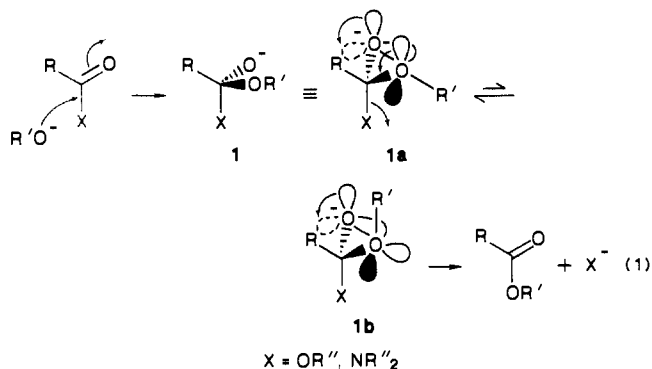
the acyl carbon will yield the tetrahedral intermediate 1. In the stereoelectronic theory, breakdown of this intermediate with cleavage of the C–X bond is facilitated by two nonbonded electron pairs oriented app (shaded) to the C–X bond in conformation 1a. In conformation 1b only one nonbonded electron lone pair is oriented app to the scissile C–X bond. In the stereoelectronic theory, cleavage of the C–X bond of the tetrahedral intermediate 1 is presumed to be controlled by the number of app lone pairs and thus should proceed through conformation 1a rather than 1b.

The stereoelectronic effect is considered to arise from the mixing of a lone-pair orbital with the antibonding σ^* of an adjacent polar bond,[11,12] such as the C–X bond of the tetrahedral intermediate 1. As we will see, molecular orbital calculations have provided theoretical justification for the stereoelectronic, orbital interactions depicted in 2 for tetracovalent carbon and phosphorus and pentacovalent phosphorus species.[6–11,13,14,17–22] An alternative classical resonance description of this orbital interaction can be viewed in terms of contributions from a double-bond–no-bond resonance structure as in 3.


3
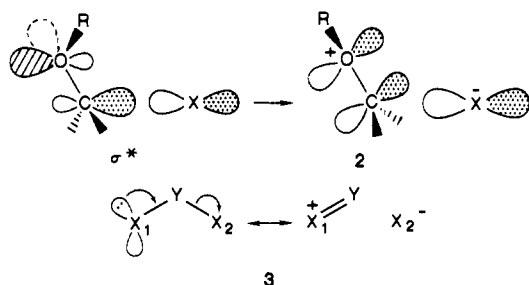
In this review I describe the current theoretical understanding of the Deslongchamps stereoelectronic theory, provide examples of its application in simple carbon and phosphorus bioorganic "model" systems, and then describe applications of these concepts to biological systems. A number of the examples discussed in this review have been drawn from work in my own laboratory. Our concern with the stereoelectronic effect will be limited largely to those systems influenced by the orientation of lone electron pairs, although many other conformationally dependent orbital interactions will quite likely perturb the ground-state structure and reactivity of molecules. Several excellent monographs on the stereoelectronic effect in organic chemistry[2,3] have recently appeared, and no effort will be made in this review to extensively duplicate the excellent coverage of these areas by Deslongchamps[2] and Kirby.[3] In

addition, Taira and Gorenstein[23] also recently reviewed the area of stereoelectronic effects in organophosphorus chemistry.
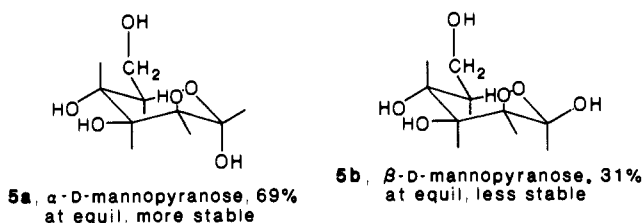
II. Ground-State Stereoelectronic Effect: The Anomeric Effect

A. Carbocyclic Rings

The stereoelectronic effect has long been believed to provide the best explanation for the anomalous ground-state structures and energies of carbohydrates.[24,25] In contrast to the behavior of substituted chair conformation cyclohexanes, where axially substituted six-membered rings 4a are higher in energy

4a   4b
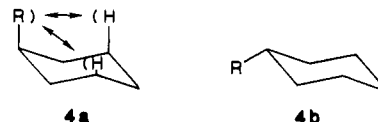
than equatorially substituted systems 4b, in various pyranoses 5 the relative energies of the two C-1 anomeric epimers are reversed with the axial epimer, such as the α anomer of mannose 5a, now lower in energy than the β anomer 5b. This "anomalous" behavior,

5a, α-D-mannopyranose, 69%   5b, β-D-mannopyranose, 31%
at equil, more stable   at equil, less stable

known as the anomeric effect, was first recognized by Lemieux.[26,27] It states that electronegative substituents such as alkoxy or hydroxy groups at C-1 of the pyranoses prefer the axial position in the chair conformation of the pyranose ring, despite the steric effect that should destabilize this conformation. In fact, the size of the alkoxy group in 2-alkoxytetrahydropyrans 6 has little

6
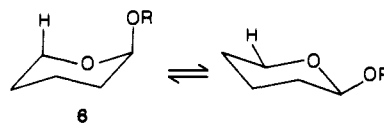
effect on the anomeric preference[28,29] for the axial position. In chloroform solution, 2-methoxytetrahydropyran (6, R = Me) is largely in a chair conformation with an axial methoxy group (77–82%). Even the sterically bulky tert-butoxy group in 2-tert-butoxytetrahydropyran (6, R = t-Bu) is predominantly (62%) in the axial position. On the other hand, the electron-withdrawing ability of the substituent serves as a good guide to the relative axial anomeric preference for the substituent:[30]

halogen > PhCOO > AcO > AcS > MeO > RS >
                                       HO > NH$_2$ > MeOOC
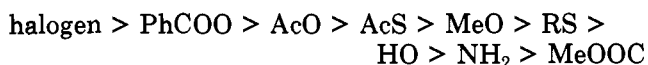
This effect of substituent electronegativity is consistent with the n $\leftrightarrow$ σ^* orbital interaction depicted in 2 and believed responsible for the stereoelectronic anomeric effect. The partial transfer of electron density from a heteroatom to another heteroatom will be enhanced if the latter heteroatom is more electronegative.
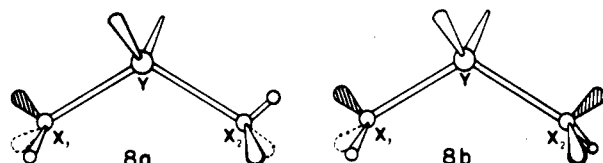
Figure 1. Conformations g,t (8a) and g,g (8b). Dihedral angles about the X_1-Y and X_2-Y bonds are defined by the X_1YX_2 structural fragment and are gauche (g, dihedral angle $\pm 60°$) or trans (t, dihedral angle $180°$). For $X_1 = X_2 =$ divalent oxygen, the sp^3-hybridized lone pairs are also shown with the antiperiplanar lone pairs being shaded).

As will be described in the theory section later, this two-electron orbital interaction is stabilizing.

Another view of the anomeric effect that has been popular over the years emphasizes the conformational dependence to the electron pair–electron pair (or dipole–dipole) repulsion[25,31] (7). This "rabbit ear effect"[32]
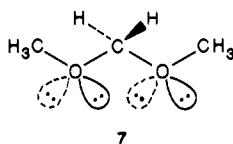
will be especially destabilizing when the lone-pair orbitals are eclipsed, and thus the staggered conformation with lone pairs app to adjacent polar bonds will minimize this destabilizing four-electron interaction. Although all of these orbital interactions (stabilizing and destabilizing) contribute to the anomeric and stereoelectronic effect, currently most theoretical studies have emphasized the stabilizing two-electron two-orbital interaction as the main contribution to these conformational energy differences. As pointed out by Wolfe,[24a] the rabbit ear effect likely is an example of the "Harvey effect".[24b] Various experimental estimates of the magnitude of the anomeric effect have been made, and a value of 1.4–1.5 kcal/mol for the preference of an axial alkoxy group in cyclic acetals appears to be reasonable.[33,34]

B. Ground-State Stereoelectronic Effects on the Conformation of Six-Membered-Ring Phosphorus Heterocycles

The anomeric effect is also observed in other XYX (Figure 1) heteroatom molecular systems, as for example, phosphate esters (X = OR, Y = PO_2). As discussed above, it is energetically more favorable to have a conformation about a P–O bond that allows an oxygen lone pair to be antiperiplanar (app) to an adjacent polar bond (P–OR). This again is a reflection of the ground-state stereoelectronic (anomeric) effect:[7-10,17,19] favorable $n_O \leftrightarrow \sigma^*_{P-OR}$ two-electron interactions in the ground state. Thus 2-phenoxy-1,3,2-dioxaphosphorinane (9) is largely present in solution with the phenoxy
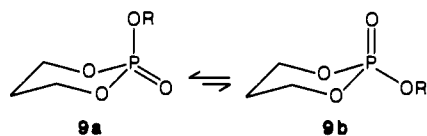
group axial.[35] This stereoelectronic, ground-state axial preference for the methoxy group in a phosphate ester is so strong that the trans isomer of 5-*tert*-butyl-2-methoxy-1,3,2-dioxaphosphorinane is shown by X-ray crystallography[29] to exist in the sterically unfavorable

(but anomerically favorable) diaxial conformation 10.

diequatorial 10

diaxial (favored) 10
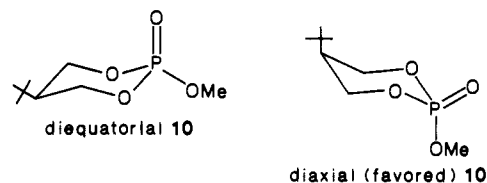
Our laboratory and others have also provided additional support for these unusual conformational preferences in solution.[36-41] The conformational and configurational analysis[36-38,42-54] of phosphorinanes (e.g., 11–14) has been based upon ^{31}P chemical shifts,[38,45]

a (11-14)

b (11-14)

Ar: 11, *p*-MeOPh; 12, Ph; 13, *p*-NO$_2$Ph; 14, 2,4-(NO$_2$)$_2$Ph
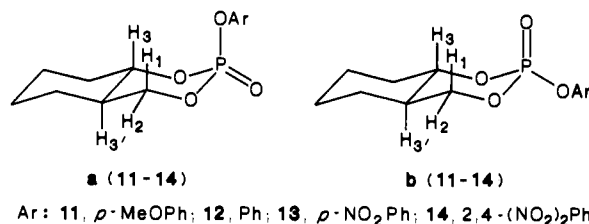
$^3J_{HCOP}$ coupling constants,[35,55,56] and P=O stretching frequencies.[51-54,57] Again all of the trans isomers are in a chair conformation with an axial ester bond. This is the conformation that maximizes the $n_O \leftrightarrow \sigma^*_{P-OR}$ interaction (ground-state stereoelectronic, anomeric effect).

Coupling constants as well as ^{31}P chemical shifts for the cis isomer of the phosphoramidate 15b are quite unusual with $^3J_{H(1)P}$ (=13.6 Hz; see structures 11–14 for numbering convention) being larger than $^3J_{H(2)P}$ (=8.8 Hz) and a ^{31}P chemical shift upfield (by 0.25 ppm) of 15a.[23,36,37] These values are inconsistent with a chair

15a   15b
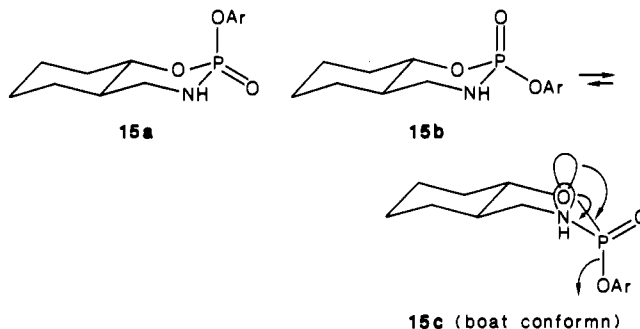
15c (boat conformn)

conformation, which should have a single large $^3J_{H(2)P}$ coupling constant of ~24 Hz and $^3J_{H(1)P}$ and $^3J_{H(3)P}$ coupling constants of ~0 Hz, as observed for the trans isomer, and suggest that the cis isomer is in a twist–boat conformation for the phosphorinane ring.[36,37] The large $^3J_{H(3)P}$ (=11.5 Hz) and $^3J_{H(1)P}$ (=13.6 Hz) coupling constants require nongauche dihedral angles (H_3COP and H_1CNP) and hence a nonchair conformation. By flipping from the chair conformation 15b to the twist–boat conformation 15c, the equatorial bond moves into a pseudoaxial position. The anomeric preference for this axial conformation is likely the basis for the unique *ground-state* twist-boat distortion in this ring system. The conformation represents a balance between the stereoelectronic anomeric effect favoring the axial orientation in the twist-boat and the 1,4-steric and eclipsing interactions favoring the chair conformation.

The percent twist-boat for each equatorial epimer can be calculated from an analysis of these coupling constants and ^{31}P chemical shifts,[36,37] and values are listed

compd	^{31}P chem shift diff, ppm	% twist-boat calcd a	% twist-boat calcd b	equil^c $\Delta\Delta G_0$	hydrolysis^d $\Delta\Delta G^*$
11	2.36	46	48	1.81	1.08
12	2.38	46	47	1.73	1.17
13	2.13	50	53	1.95	1.47 (1.27^e)
14	0.69	100	85	1.85	1.44
15	-0.25	100	100	1.45	0.75
16	4.5	0	0	2.3	1.06^e

^{a} Derived from coupling constants. ^{b} Derived from ^{31}P chemical shift differences. ^{c} In 100% DMF at 30 °C (kcal/mol). ^{d} In 75% dioxane/water, 70 °C (kcal/mol). ^{e} In 12% methanol/water, 30 °C (kcal/mol).

in Table I. Note that the percent twist-boat conformation increases with the increase of electronegativity of the substituents on the aromatic ring, as expected from the more favorable $n_0 \leftrightarrow \sigma^*_{P-OAr}$ interaction in the twist-boat conformation, with the increase in polarity of the P–OAr bond.

Similar analysis[58] of the coupling constants and ^{31}P chemical shifts has established that the cis ester 16b is in a chair conformation in contrast to the esters 11b–14b. The chair conformation for 16b is also sup-

16a

16b
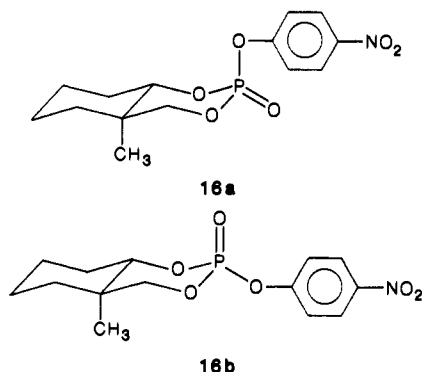
ported by the equilibrium results shown in Table I. At 30 °C in DMF, 13b is 1.95 kcal/mol higher in energy than 13a. However, this energy difference is greater in the case of the 16a/16b pair: 16b is 2.3 kcal/mol higher in energy than 16a. As discussed above, 13b prefers to be in a twist-boat conformation because of the ground-state (anomeric) stereoelectronic effect compensating for the torsional strain in the twist-boat conformations. Since this ring-flipping to form twist-boat conformations is sterically more destabilizing in the case of 16b, with very unfavorable boat bowsprit interactions between the C(4) ring-junction methyl group and P(2), it is higher in energy than 13b.

III. Theoretical Basis for the Stereoelectronic Effect

A. Mulliken Overlap Population Analysis on X_1YX_2 ($X = O, N; Y = P, C$)

Molecular orbital calculations[6–14,17–21] on the X_1YX_2 ($X = O, N; Y = P, C$) structural fragments (Figure 1) have shown that the X_1–Y bond is strengthened (as indicated by an increase in the Mulliken overlap population) while the Y–X_2 bond is weakened when the X_1 atom lone pair is app to the Y–X_2 bond (structure 8,

SCHEME I
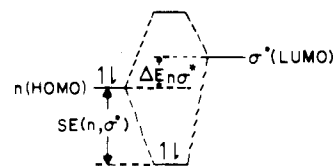
Figure 1). In the gauche,trans (g,t) conformation of dimethoxymethane [structure 8a ($X = OCH_3$, $Y = CH_2$)] the overlap population for the trans C–O ($Y = C$, $X_2 = O$) bond is 0.022 electron lower than the overlap population for the gauche C–O bond. As shown in Figure 1 and in structures throughout this review, the stereoelectronic effect is most conveniently analyzed in terms of the orbital interactions involving sp^3-hybridized lone-pair orbitals. Comparable analysis with nonequivalent σ- and π-character orbitals of sp^2-type hybridized atoms is also possible. Because the σ- and π-type lone-pair orbitals are of similar energy (relative to the much higher antibonding orbitals), they both mix effectively and analysis in terms of sp^3-hybrid orbitals gives comparable results.[3]

One lone pair n_{X_1} on X_1 (17) is properly oriented only in the gauche bond (X_1–Y of 17) to allow the maximal overlap (in phase) with the antibonding $\sigma^*_{Y-X_2}$ of the adjacent polar bond (Y–X_2). Since the bonding orbital

17
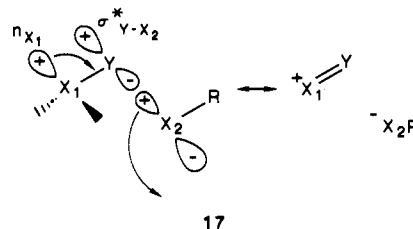
σ_{X_2-R} in the trans bond (Y–X_2 of 17) is app to X_1 and in phase with the adjacent antibonding $\sigma^*_{X_1-Y}$ orbital, none of the lone pairs n_{X_2} on X_2 can as effectively mix with the antibonding $\sigma^*_{X_1-Y}$ orbital of the adjacent polar bond (X_1–Y). Thus, because the lone pairs on X_2 cannot effectively overlap with the antibonding orbital $\sigma^*_{X_1-Y}$, there is little of the stereoelectronic orbital interactions from lone pairs on X_2.

On the basis of one-electron molecular orbital theory,[59] the two-electron stabilization energy (SE) resulting from the interaction of a doubly occupied MO (ξ) with a vacant nondegenerate MO (σ^*) may be approximated as being inversely proportional to the energy separation of the two MO's and directly proportional to the square of their overlap (eq 2). In the above example the

$$SE(\xi, \sigma^*) \propto \frac{S_{\xi\sigma}^2}{\Delta E_{\xi\sigma^*}} \qquad (2)$$

doubly occupied MO (ξ) is the nonbonding orbital ($\xi = n_{X_1}$) on X_1 and the vacant nondegenerate MO (σ) is the antibonding orbital ($\sigma^* = \sigma^*_{Y-X_2}$) of the adjacent polar bond. From eq 2, this stabilization energy [SE-(ξ, σ^*)] increases with increasing overlap ($S_{\xi\sigma^*}$) and decreasing energy separation ($\Delta E_{\xi\sigma^*}$) between the interacting orbitals (Scheme I).

The lone-pair stereoelectronic effect presumably derives from this orbital interaction, and as indicated by eq 2, maximal overlap between N and σ^* is found for the app orientation.[59] (Of course although other orbital

interactions, including destabilizing four-electron orbital interactions will be involved as well,[59] the two-electron stabilization effect generally dominates.)

In the g,t-dimethoxymethane, one lone pair (shaded in **8a**) on the gauche-bond oxygen is app to the trans C–O bond, while no lone pairs on the trans bond oxygen are app to the gauche bond. Thus, the $Y–X_2$ bond is weaker and predictably longer than the $X_1–Y$ bond because it has one app lone pair on X_1 and no lone pairs on X_2 app to the $X_1–Y$ bond.[17,18,19] Similarly, in the g,t conformation of dimethyl phosphate monoanion (structure **8a**, X = OCH_3, Y = PO_2^-) the overlap population for the longer trans P–O bond ($Y–X_2$) is 0.017 electron lower than the overlap population for the shorter gauche P–O bond ($X_2–Y$).[17-19] Lehn[6-10] and Pople[11,12] and co-workers have shown similar overlap population differences in related systems.

X-ray crystal structures of various acetals,[12] phosphate esters,[60] and related molecules[3] have largely shown the same pattern of bond lengths consistent with the theoretical predictions of the stereoelectronic orbital interactions. Thus, as shown in the structure of 1,2-dichlorodioxane (**18**), the axial chlorine bond is con-

18
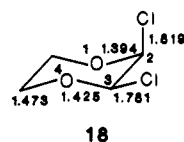
siderably longer than the equatorial bond and the $O_1–C_2$ bond is shorter than the $O_4–C_3$ bond.[3] It is difficult to rationalize this pattern of bond length changes on the basis of electron–electron or dipole–dipole repulsion (the rabbit ear effect)[25,31,32] (**19a/b**). The strengthening

19a **19b**
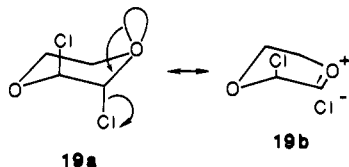
and shortening of the $X_1–Y$ bond and the lengthening and weakening of the $Y–X_2$ bond in **8** support the classical description of the stereoelectronic effect in terms of the double-bond–no-bond resonance structure as in **19a**. Jones and Kirby[60] have also shown that the C–O bond lengths in 2-substituted (aryloxy)tetrahydropyran derivatives increases with an increase in the electronegativity of the aryl group.

B. Theoretical Calculations on Acyl Addition/Elimination Reactions

A number of molecular orbital calculations[6-12,17-19] have supported the existence of the operation of the stereoelectronic effect in tetrahedral carbon species. Many of these calculations were based only on overlap population and energy differences in stable molecular structures that, as described in a later section, tend to minimize the impact of the stereoelectronic effect. Calculations have suggested that stereoelectronic effects play a major role in the relative energies of transition states, much more so than on ground states or intermediates. It is thus important to use calculated transition-state energies as a guide in the evaluation of the stereoelectronic effect. Recently, quantum mechanical studies have detailed the reaction profile for the ad-
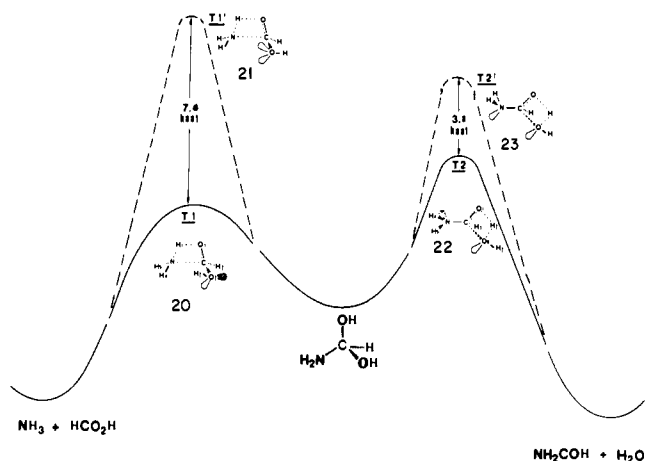
Figure 2. Reaction profiles for acyl addition/elimination reaction (3) are shown assuming various conformations about the C–N and C–O_2 bonds. Reproduced with permission from ref 62.

dition/elimination reaction 3 between ammonia and formic acid, proceeding via a tetrahedral intermediate.[13,61,62]

$$NH_3 + HCO_2H \rightarrow H_2NCH(OH)_2 \rightarrow$$
$$NH_2CHOH + H_2O \quad (3)$$
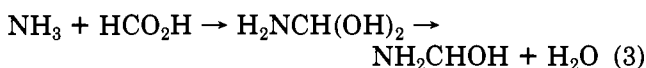
Shown in Figure 2 are the reaction profiles for formation of the amide bond in the reaction of ammonia and neutral formic acid. The profiles differ with respect to the conformations about the C–N and C–O_2H bonds. (Dihedral angles about the C–N and C–O_2 bonds are defined by the $H_5NCO_2H_2$ structural fragment. In **20** and **21** the dihedral angle $H_5N–CO_2$ is actually closer to anticlinal (120°) although it is characterized for comparison with structure **8** as trans. In **22** and **23** the dihedral angle NCO_2H_2 again is roughly anticlinal, although it is characterized as trans.) All four conformers (**20–23**) have been optimized as clear transition states, as indicated by a single negative quadratic force constant. As expected from an anomeric-type, double-bond–no-bond resonance contribution, the overlap population of a bond that is app to a lone pair is smaller than the overlap population of a bond that is not app to a lone pair (assuming we are comparing otherwise identical structures). Thus, the C–N overlap population is 0.264e in the **21** conformation, whereas it is 0.229e in the **20** conformation.[62] The presence of an app lone pair to the scissile C–N bond in the **20** conformation weakens this bond (reduces the overlap population). As expected from the double-bond–no-bond resonance description of the stereoelectronic effect, the C–O_2 overlap population in **20** (0.540e) is larger than in **21** (0.490e). The app lone pair on O_2 to the C–N bond in **20** imparts some double-bond character to the C–O_2 bond. Similar overlap population stereoelectronic effects are observed for the **22** and **23** conformations (Scheme II).

It should be easier to break (or make, by microscopic reversibility) the bond that possesses no-bond character, and indeed as shown in Figure 2, this has been confirmed in these calculations. For the addition transition state (formation of the C–N bond), the conformation **20** with an oxygen lone pair on O_2H app to the C–N bond is 7.4 kcal/mol lower in energy than **21** which has no lone-pair orbital on O_2 to the C–N bond. Note in the following discussion we ignore the lone-pair orbitals

SCHEME II

Figure 3. Reactions profiles for hydroxide-catalyzed hydrolysis of dimethyl phosphate. The reaction coordinate is defined by the P–OH distance (d_{OH} and P–O2CH$_3$ distance (d_{POCH3}) for the attack and displacement steps, respectively. The solid line represents the profile for ⁻OH attack on g,g DMP to yield g,g,g⁻ DMPanes (□) and for ⁻OH attack on g,t DMP to yield t,g,g⁻ DMPanes (●). The dashed line represents the profile for ⁻OH attack on g,t DMP to yield g,t,t DMPanes (▲).

on O$_1$, which will also be app to the C–N or C–O$_2$ bonds and hence stereoelectronically facilitate both C–N and C–O$_2$ bond translation. As Deslongchamps proposed,[1,2] selective bond cleavage in a tetrahedral intermediate requires at least two antiperiplanar lone pairs. Similar stereoelectronic effects operate on the second transition state, involving the water elimination step. The conformation 22 with a nitrogen lone pair app to the scissile C–O$_2$ bond is 3.1 kcal/mol lower in energy than 23, which has no lone-pair orbital on nitrogen app to the scissile C–O$_2$ bond.

In conclusion, the stereoelectronically most favorable transition state is one that possesses a lone pair app to the adjacent scissile bond while at the same time does not have a lone pair on the cleaving atom app to a polar adjacent bond (26).
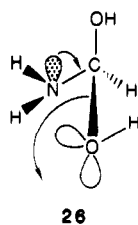
Lehn and Wipff reached similar conclusions[7-10] based upon molecular orbital calculations of overlap populations and energy differences in tetrahedral intermediates. These results also support the operation of stereoelectronic effects on the mechanism of action of serine proteases originally proposed by Bizzozero et al.[23,63,64] We will come back to this application of the stereoelectronic effect to the mechanism of serine proteases in section VA.

C. Theoretical Calculations of Hydrolysis Reaction Profiles of Phosphate Esters

Shown in Figure 3 is the reaction profile[14,19] for the base-catalyzed hydrolysis of dimethyl phosphate (DMP) in two different ester conformations (eq 4).

$$(CH_3O)_2PO_2^- + {}^-OH \rightarrow [(CH_3O)_2PO_3H]^{2-} \rightarrow$$

27

$$CH_3OPO_3H^- + CH_3O^- \quad (4)$$

For dimethyl phosphate 27 in a gauche,gauche (g,g) conformation, attack of ⁻OH opposite one of the methoxyl ester bonds can produce only one possible mode of attack, yielding a g,g,g⁻ transition state [torsional angles about the P–OMe bonds are defined by the MeOPOMe structural fragment and the torsional angle

about the P–OH bond is defined by the MeO(+)POH fragment. Conformations g,g,g⁻, t,g,g⁻, and g,t,t are shown with antiperiplanar lone pairs shaded)] and the corresponding dimethoxyphosphorane (DMPane) intermediate 28. In contrast, attack of ⁻OH opposite one

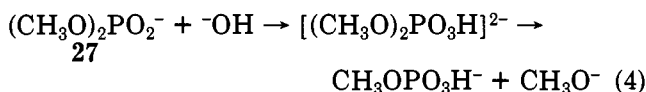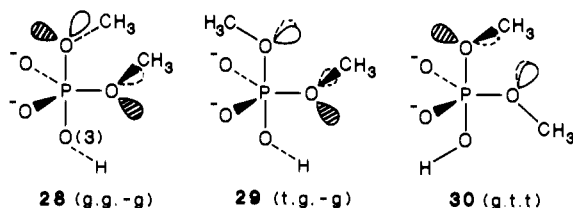of the methoxy ester bonds in the gauche,trans (g,t) DMP structure 27 can proceed via two different reaction paths. Thus, ⁻OH attack opposite the gauche methoxyl ester bond produces a g,t,t transition state and g,t,t DMPane intermediate 30. Attack of ⁻OH opposite the trans bond produces a t,g,g⁻ transition state and g,t,t DMPane intermediate 29.

As shown in Figure 3, for all conformations, the reactions are computed to proceed via a metastable pentacovalent intermediate with separate transition states for the (hydroxide) addition and (methoxide) elimination steps. Most significantly, the energy of the transition states is very dependent upon the conformation about the basal methoxyl bond. For the methoxide elimination step, the transition states with a basal gauche methoxyl group (the t,g,g⁻ or g,g,g⁻ structures), 29, are ca. 11 kcal/mol lower in energy than the transition state with a trans basal methoxyl group (the g,t,t structure), 30. This result agrees nicely with the stereoelectronic theory. As can be seen in the t,g,g⁻ (29) or g,g⁻,g (28) structures, the basal gauche methoxyl group has one additional lone pair (shaded), which is antiperiplanar (app) to the breaking methoxyl bond, than that of the g,t,t (30) structure in which no lone pair of the basal trans methoxyl group is app to the breaking methoxyl bond. This additional weakening of the apical methoxyl bond by an app lone pair on the basal methoxyl oxygen is suggested to be attributable to the stereoelectronic effect mixing of the nonbonding app

lone pair with the antibonding σ^* apical orbital (31–33).

31

32

33
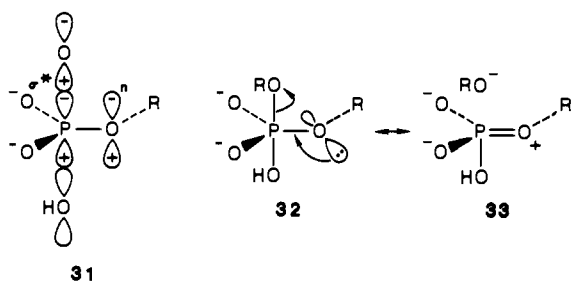
The effect may again be viewed within the classical resonance description, rather than the above perturbational scheme. In this classical, "anomeric"-type picture the no-bond–double-bond resonance structure **33** presumably significantly contributes to the transition-state structures. These considerations suggest that an axial P–O ester bond app to a lone pair on the basal oxygen should be weakened and should have a reduced overlap population. The basal ester bond with the oxygen atom bearing the app lone pair is strengthened and has an enhanced overlap population.

Similarly, stereoelectronic control of the ⁻OH attack transition state is apparent from Figure 3. To describe the app interactions in the ⁻OH attack step we must relabel the torsional angles of the basal ester relative to the translating apical bond. Thus, in the g,t,t (**30**) structure, the basal ester bond is *cis to the P–OH bond*. In the t,g,g⁻ (**22**) and g,g,g⁻ (**28**) structures the dihedral angle between the basal methoxyl bond and the apical OH bond is 120° or anticlinal (ac). Significantly, for the ⁻OH attack step, conformer **30** is at least 4.0 kcal/mol lower in energy than **28** or **29** transition states. The lower energy for the cis transition state relative to the ac transition state indicates[14,17] that two partially app lone pairs (from a cis basal bond) are nearly as effective as a single app lone pair (from a gauche basal bond) in facilitating bond translation. These conclusions for the attack step actually follow directly from a consideration of the principle of microscopic reversibility. Since ⁻OH is chemically similar to ⁻OCH₃, stereoelectronic effects altering the activation energy for ⁻OH translation (attack or displacement) must be nearly identical with stereoelectronic effects in ⁻OCH₃ translation (displacement or attack).

As indicated previously, besides weakening the bond adjacent to the app lone pair, the stereoelectronic effect will strengthen the bond containing the app lone pair[7–10,17–19] (we have termed this is a "counterbalancing" stereoelectronic effect). The orientation of both the nontranslating and translating axial bond is generally not very important in determining the relative transition-state energies for the hydrolysis of DMP. Thus, in the transition state for methoxyl leaving in reaction 4, it is found that orientation of lone pairs on the axial methoxy group does not affect the energy of the transition state. If a lone pair on this axial oxygen were app to the basal methoxyl bond, the bond containing the app lone pair has some double-bond character to it (**34**). The double-bond contribution should increase the axial bond overlap population and presumably strengthen this bond.

The reason that the transition-state energies in the phosphoranes are insensitive to the translating axial bond conformation likely reflects the difference in bond

34
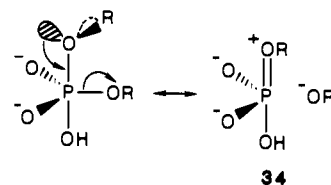
lengths between the basal and the scissile axial bonds. The basal methoxyl bond length is 2.50 Å. The orbital interaction picture for the counterbalancing stereoelectronic effect requires effective overlap of the nonbonding lone-pair orbital on the axial methoxyl oxygen with the basal methoxyl σ^* orbital. Increasing the separation between phosphorus and the oxygen atom bearing the lone pair will diminish this overlap, $S_{n\sigma^*}$, reduce the stabilization energy of eq 2, and reduce the counterbalancing stereoelectronic effect. On the other hand, increasing the distance between phosphorus and the axial oxygen should lower the energy of the axial σ^* orbital and hence decrease the energy separation, $\Delta E_{n\sigma^*}$, and increase the stereoelectronic effect produced by the normal stereoelectronic effect (see eq 2 and Scheme I).

Experimental evidence[65–67] in support of the calculated reaction profiles for hydroxide-catalyzed hydrolysis of phosphate esters will be given in section IVC.

D. Manifestation of the Stereoelectronic Effect in the Transition State

As described earlier, the orbital interactions responsible for the stereoelectronic effect are expected to be magnified in transition state structures.[17–19] While ground-state stereoelectronic effects can be quite modest (1 or 2 kcal/mol), transition-state stereoelectronic effects can be considerably larger and hence significant kinetic accelerations might be observed in suitably designed systems. In the above section, it was shown that the interaction of a doubly occupied MO (such as the app lone-pair orbital ξ = n) with a vacant MO (such as the antibonding orbital σ^*) yields a two-electron stabilization energy (eq 2). From eq 2 this stabilization energy increases with increasing overlap, $S_{n\sigma^*}$, and decreasing energy separation, $\Delta E_{n\sigma^*}$, between the interacting orbitals. Thus, the energy differences between the conformations of the ground state, intermediates, or transition states of the hydrolysis reaction of dimethyl phosphate (reaction 4, section IIIC) vary in a manner consistent with the stereoelectronic effect and eq 2. In dimethyl phosphate the energy difference between the conformations is <1 kcal/mol.[46] In the pentacovalent metastable dimethyoxytrihydroxyphosphorane intermediate, the energy difference between the conformations is 2–6 kcal/mol. In the pentacovalent transition states the energy differences are 8–11 kcal/mol.[19] Of course, if the stereoelectronic effect did not have its major impact in the transition state, little activation energy differences and no kinetic acceleration would result from these interactions. From eq 2, increasing the distance between phosphorus and the leaving-group oxygen should lower the energy of the axial σ^* orbital and hence decrease the energy separation, $\Delta E_{n\sigma^*}$, and increase the stabilization energy.[17–21] In the ground state, σ^* is quite high in energy, mixing between n and σ^* via the stereoelectronic effect is minimal, and indeed as described in section II, the
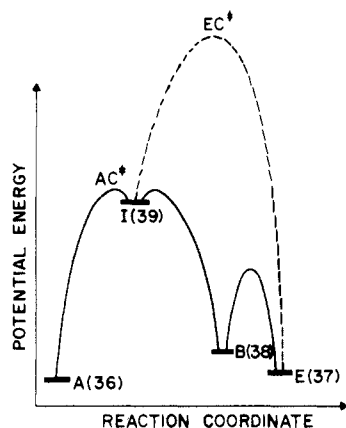
Figure 4. Schematic energy profile for the cleavage of a conformationally flexible ring system such as the aryltetrahydropyranyl acetals (e.g. 36/37) or arylphosphorinane esters (e.g. 11a/b). A and E represent the axial and equatorial chair conformation six-membered ring systems. I represents a high-energy intermediate (planar carbonium ion or pentacovalent phosphorane), B a flexible twist-boat conformation for either the tetrahydropyranyl or phosphorinane ring, and EC* the hypothetical transition state for cleavage of the X–OAr (X = C, P) of E with the ring system fixed in the ground-state chair conformation (partially derived from Kirby[70]).

ground-state anomeric effect is experimentally found to be quite small (<2 kcal/mol).

The same explanation appears to apply in tetrahedral carbon species.[18] Thus, in an ab initio molecular orbital calculation at the STO-3G basis set level, g,g-dimethoxymethane **8b** is only 0.9 kcal/mol lower in energy than the g,t-dimethoxymethane **8b**. The g,g conformation has one more app lone-pair interaction with a polar adjacent bond than the g,t-dimethoxymethane, but it leads to <1 kcal/mol of stabilization (however, this small stereoelectronic effect is still the basis for the ground-state anomeric effect). Recall in transition state 20 the lone pair is app to the elongated, scissile NH_3 bond (with lower σ^*) and is stabilized by 7.4 kcal/mol relative to the 21 transition state.

IV. Stereoelectronic Effects on Reactivity

A. Acetals and Sugars

Somewhat disturbingly, the literature on the hydrolysis of acetals such as the α and β anomers of alkyl glucopyranosides, appears to suggest that stereoelectronic effects are *not* a significant factor in influencing the relative rates of hydrolysis of isomers differing in the relative orientation of lone pairs to the leaving group. Thus, the β anomers of the glucopyranosides hydrolyze up to 3.2 times *faster* in spite of the fact that neither lone pairs on the endocyclic acetal oxygen is app to the equatorial leaving alkoxy group.[68] Similarly in 2-(aryloxy)-2-oxadecalins, the equatorial acetal also hydrolyzes 3.3 times faster than the axial isomer.[69] This study monitored the spontaneous hydrolysis of both epimers, rather than the acid-catalyzed hydrolysis in the earlier pyranoside studies. As will be discussed in section IVC, my laboratory observed a similar lack of stereoelectronic control in the hydrolysis of phosphate esters, and this failure is likely attributable to conformational flexibility in these systems. In both six-membered-ring acetals and phosphate esters, reaction of the chair equatorial epimer is likely occurring

through higher energy twist-boat conformation **35**. As

35
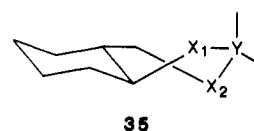
shown in Figure 4,[70] using as an example the reaction of the 2-(aryloxy)-2-oxadecalins, the axial epimer **36** can react in its ground-state conformation with stereoelectronic assistance from an app lone pair on the ring oxygen. In the chair equatorial isomer **37** there are no
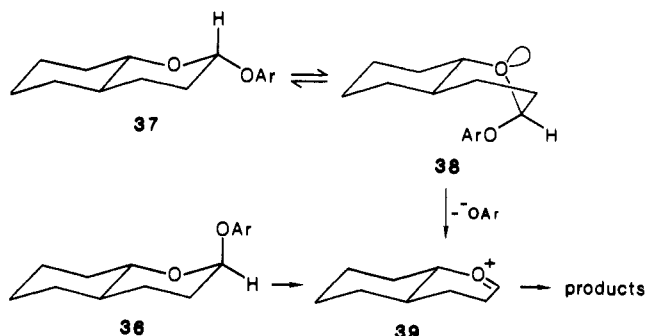
app lone pairs on the ring oxygen to stereoelectronically assist in the cleavage of the equatorial aryloxy bond. Reaction through this conformation would necessarily proceed through a high-energy transition state (EC*). In contrast, conformation **36** can react through a stereoelectronically favorable low-energy transition state (AC*). However, the twist-boat structure **38** does provide for stereoelectronic assistance, with a lone pair on the ring oxygen app to the pseudoaxial aryloxy leaving group. If conformation **38** is energetically accessible, then reaction will funnel through this conformation. All that is required is that the transition state for conformational isomerization of **37** and **38** and the stereoelectronically assisted transition state for subsequent reaction of the high-energy intermediate **38** are lower energy than the AC* transition state (Figure 4). As described above, twist-boat forms are indeed quite readily accessible because of the ground-state stereoelectronic (anomeric) effect.

A second factor is also obscuring the observation of kinetic stereoelectronic effects in these systems. As shown in Figure 4, both epimers will react via identical or similar high-energy oxocarbonium (or pentacovalent phosphorus) intermediates **39**. The transition states will therefore be quite late and similar in energy and structure to the carbonium ion or pentacovalent phosphorus intermediate.[70] The high-energy intermediates (either planar oxocarbonium or pentacovalent phosphoranes; see **70** below) "lost" all memory of the relative orientation of the lone electron pairs on the endocyclic oxygen in chair or twist-boat ground-state structures. The relative rates of reaction of the two epimers will therefore only reflect the ground-state energy differences. Because the chair equatorial epimer is higher energy than the chair axial epimer due to the ground-state stereoelectronic effect, the former epimer reacts slightly faster.

Thus, even in relatively constrained systems, the stereoelectronic effect can often be masked by the remaining flexibility in the ring structures. However, more rigid systems can provide a direct measure of the stereoelectronic barrier EC*. Kirby studied several

more highly constrained systems that avoid this alternative pathway passing through flexible forms[70] (40 and 41).
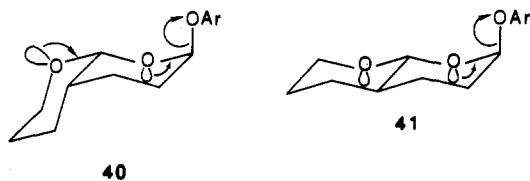
40 **41**

For example, the cleavage of the aryloxy group in bicyclic acetals 40/41 generates cation 41a, the cyclization product of the oxocarbonium ion aldehyde 41b.[70-72] Because the aldehydic oxygen is such a good leaving group, cleavage of both bonds is likely to be concerted. The orientation of lone pairs on the oxygen atom of ring B will therefore influence the rate of cleavage of the aryloxy group. In epimer 40 a lone pair on this oxygen is app to the carbon–aldehydic oxygen bond in ring A. Epimer 41 does not have a lone pair on the remote oxygen to stereoelectronically assist in the cleavage of the two bonds. It is thus significant that the spontaneous hydrolysis of this equatorial ring-junction epimer 41 is 1570 times slower than the acetal without the extra ring. Further, epimer 40 hydrolyzes 200 times faster than 41, entirely consistent with a stereoelectronic effect in the acceleration of its hydrolysis.

41a

41b
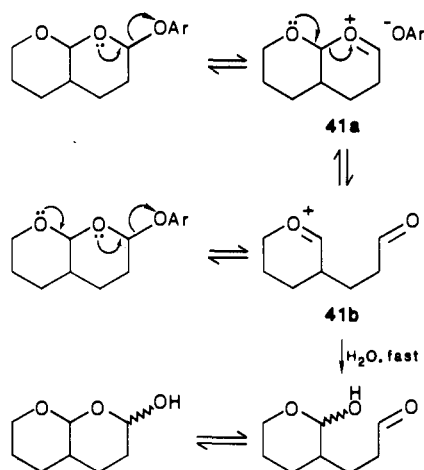
Even in the above system, sufficient conformational flexibility still exists so that the full kinetic stereoelectronic effect is still not being measured. An even more dramatic rate *retardation* due to a high stereoelectronic barrier (dashed curve of Figure 4) is demonstrated by a comparison of acetals 42 and 43. The

42 **43**
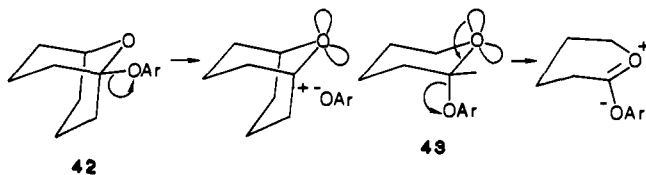
estimated difference in the rate of hydrolysis between the 2,4-dinitrophenyl esters of 42 and 43 is 1.3×10^{13}.[73] It could be argued that Kirby has now "stacked the deck", because it is well appreciated that carbonium ion 44 will have very little π overlap with the lone pairs on the ring oxygen (this can be considered a violation of Bredt's rule which does not allow bridgehead double

bonds). Planar carbonium ion 45 can have considerable π overlap and will be much more stable than 44. In

44

45
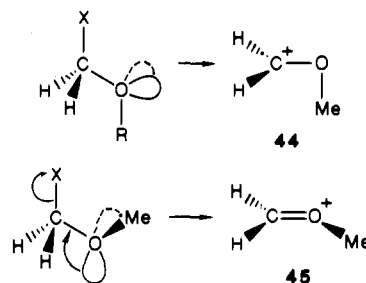
fact, it has long been recognized that oxocarbonium ions are more stable than their carbon analogue carbonium ions because of this π-electron donation from the adjacent oxygen atom.[74] The energy difference between planar and perpendicular conformations of the oxocarbonium ion $MeOCH_2^+$ is calculated to be ca. 20 kcal/mol,[74] remarkably close to the free energy of activation difference between 42 and 43 of 18.4 kcal/mol.[73] Indeed, physical organic chemists have long recognized the importance of this stereoelectronic effect, and the studies of Deslongchamps and other workers have really just recast this important concept in more general terms.

In spite of the rather strong support for the stereoelectronic effect in electron-deficient transition states and highly constrained systems, its importance in other systems has been much debated.[15,16,75-82] Much of this concern has centered around the lack of any observed kinetic acceleration in axially substituted pyranosides over the equatorially substituted epimers as discussed earlier. Sinnott and co-workers attempted to avoid the conformational flexibility problem by using pyridinium pyranosides that they believed locks the conformations more strongly than alkoxy or aryloxy pyranosides through the operation of a "reverse" anomeric effect and the increased steric bulk of the pyridine group.[16] Sinnott and co-workers[82] interpret their data to support the principle of least nuclear motion and against the stereoelectronic effect. Their arguments, however, are not very compelling, again because of the possibility of substantial conformational flexibility in their monocyclic systems. These concerns are real, however, and emphasize again that simple application of the Deslongchamps antiperiplanar lone-pair theory to flexible systems must be viewed with skepticism. Fortunately in our later applications of this theory to enzymatic systems, we may take refuge in the safe harbor of a constrained active site.

B. Stereoelectronic Effects in Esters and Amides and Related Compounds

Deslongchamps[1,2] and Kirby[3,70] provided numerous examples of the operation of the stereoelectronic effect at the acyl level of oxidation, and only a representative sampling of this work will be reviewed here. Some of the key experimental evidence supporting stereoelectronic control in the breakdown of specific bonds in tetrahedral intermediates has been provided by the acid-catalyzed hydrolysis of orthoesters to hydroxy esters.[1,83] Acid-catalyzed hydrolysis of bicyclic orthoesters 46–48 yields the same hydroxymethyl ester 49 while the orthoester 48 gives the hydroxyethyl ester 50. The first stage of this reaction is loss of the axial alcohol

46: R′ = CD₃, R = CH₃
47: R′ = C₂H₅, R = CH₃
48: R′ = CH₃, R = C₂H₅

49: R = CH₃
50: R = C₂H₅

51

SCHEME III

52A   **52B**   **52C**

53A   **53B**   **54**

SCHEME IV

52C ⟶ 54 ⟶

(R = H)

57

58
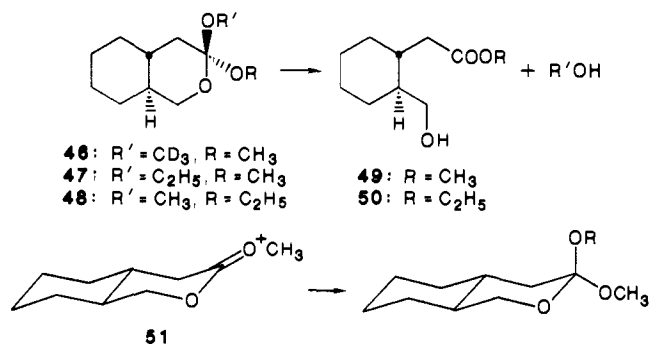
to yield the lactonium salt **51**. Deslongchamps also showed that the microscopic reverse of this reaction, namely the addition of alcohol to the lactonium salt, proceeds with the same stereospecificity.[1] Lone pairs on each of the oxygens in conformations **52A–C** stereoelectronically control the loss (or addition) of the axial alcohol (Scheme III). Note that only one lone pair in the orthoester can be oriented app to the equatorial alcohol **55**.

55
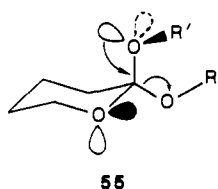
According to the Deslongchamps theory, cleavage (or attack) requires two app lone pairs and provides an explanation for the specificity in the formation and breakdown of these orthoesters.

In the next step of the hydrolysis reaction, the lactonium ion adds water to yield the hemiorthoester **56**.

56
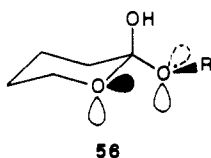
Further hydrolysis of the hemiorthoester **56** will yield by stereoelectronic principles only the hydroxy ester **57** and not the lactone **58** (Scheme IV). Lactone **58** cannot be produced because it is not possible to have two app lone pairs to the equatorial alcohol, and as in the case of the orthoester, this bond is not cleaved. However, in **52C**, two lone pairs on the exocyclic oxygens can be oriented app to the ring C–O bond, and thus stereoelectronic control control yields *only* the hydroxy ester **57**.[1,83]

This analysis can nicely explain the stability of **59**.[84] Note that **59** is locked into a conformation that does not provide for the required two app lone pairs to any of the orthoester bonds.

59
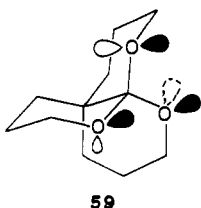
Perrin and co-workers[15,85] suggested that the orthoester results in the six-membered ring systems, which while consistent with the stereoelectronic effect can also

SCHEME V

60A   slow?   **60E**

62 (n=6)   **61** (n=6)

-EtOH
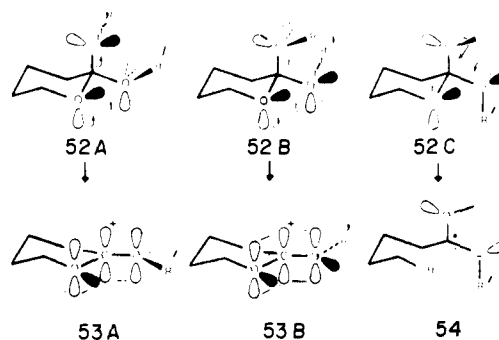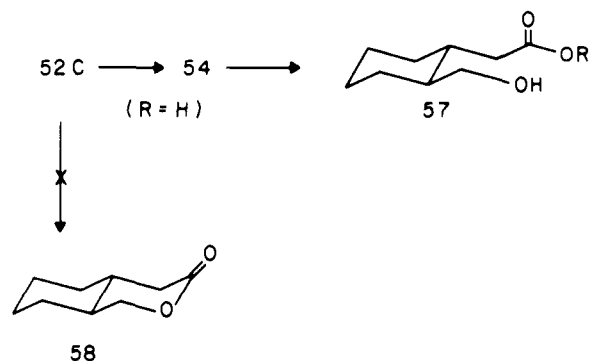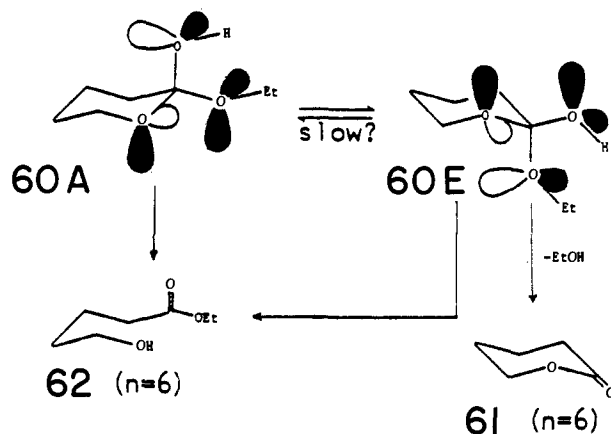
be more simply explained by the relative instability of lactones and E (syn periplanar conformation) esters.[15] Similar results are observed in the acid-catalyzed hydrolysis of monocyclic five- and six-membered orthoesters[83,86] **60–62**, where only the hydroxy ester product

62   **60**   **61**   + EtOH
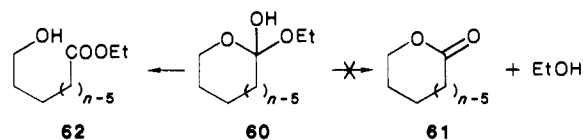
62 and none of the lactone 61 is observed, consistent with the stereoelectronic effect requirement for two app lone pairs to the breaking bond. Because lactone 62 is predicted to be the thermodynamically favored product, the stereoelectronic effect results of Deslongchamps would appear to be especially compelling. Many other examples of this type of stereoelectronic control have been demonstrated, as described earlier[1,2,3] for acetals, as well as esters, amides, hemiorthoesters,[87] hemiorthothiolates,[88] and hemiorthoamides.[89]

As pointed out by Perrin[15,85] in these five- and six-membered ring systems, a key requirement in the Deslongchamps theory is that ring inversion in intermediate 60 is slow relative to its breakdown (Scheme V). In the monocyclic ring systems, inversion of the ring from conformation 60A to conformation 60E now provides two app lone pairs to the ethoxy leaving group. Lactone 61 is thus as favorable a product based upon stereoelectronic principles as hydroxy ester 62. In order for the stereoelectronic effect to provide an explanation for the formation of only 62, ring inversion must therefore be slow. With ring-inversion rate constants[90] in cyclohexanes of 10^5–10^6 s^{-1}, the rate constant for breakdown of 60 would have to be $>10^6$ s^{-1}. While such rate constants are not unreasonable,[91] some rate constants have been measured to be much slower (ca. 10 s^{-1}).[92] An alternative explanation, that ring inversion in six-membered-ring orthoesters is much slower than that of cyclohexanes, has been ruled out by Perrin and Nuñez.[93] Apparently the inversion barrier in 2,2-dimethoxyoxane (63) is 1.4–2.1 kcal/mol *lower* than that for various cyclohexanes. It is interesting that the lower barrier to inversion is likely attributable to a stereoelectronic effect. The n $\leftrightarrow$ σ^* mixing is best in the half-chair transition state. Most significantly, ring inversion in the five-membered ring system 60 ($n = 5$) is much faster (inversion rate $>10^{12}$ s^{-1})[94] than breakdown of the intermediates ($\sim 10^8$–10^9 s^{-1}).[95] These results have thus raised some concerns about the validity of some elements of the Deslongchamps assumptions and theory.[75-78,80,81]

Perrin and co-workers proposed more stringent tests of the stereoelectronic effect theory by studying the hydrolysis of cyclic amidinium ions 64, which proceeds through the hemiorthoamide 65.[75] Unlike the hy-

drolysis of orthoester 64, which is expected to yield the more stable hydroxy ester 62 rather than lactone 61, in the case of the hydrolysis of the cyclic amidinium ion 64 the stereoelectronically predicted product, the amino amide 66 is the thermodynamically *less* stable product. Perrin and Arrhenius[15] in fact observed amino amide 66 and not lactam 67 as the kinetic product ($\geq$98:2) fully in accord with the Deslongchamps stereoelectronic control theory.
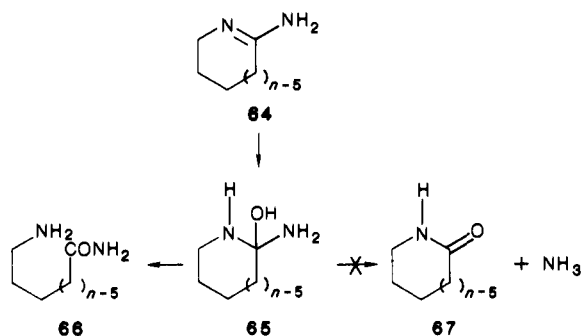
Even this test was still ambiguous because of a mismatch in the leaving-group ability of NH$_3$ vs. a primary amine. The more basic primary amine in the unsymmetrical amidine is expected to be preferentially cleaved and could be a factor in the results observed in the hydrolysis of the cyclic amidinium ion 64. Perrin and Nuñez[85] recently further tested the stereoelectronic control theory by hydrolyzing a series of cyclic six-membered-ring amidines 68 with matched leaving-
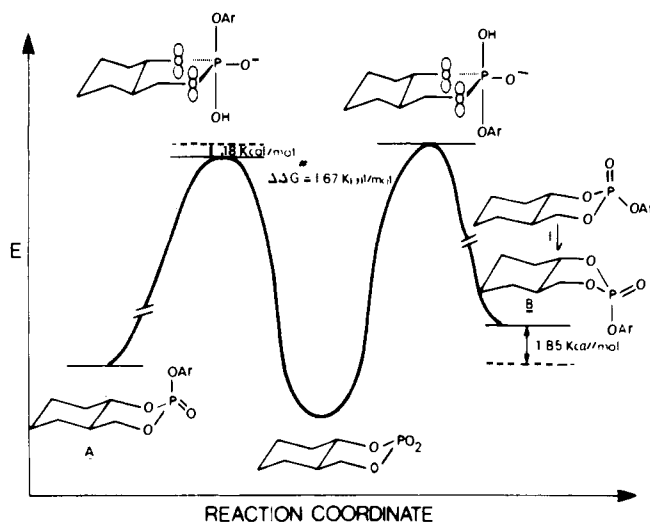
Figure 5. Reaction diagram for hydrolysis of epimeric phosphorinanes. Reproduced with permission from ref 37. Copyright 1980 American Chemical Society.

group ability and again, though not as dramatically, observed only 3–7% lactam 69a, with the remainder amino amide 69b, in confirmation of the stereoelec-

tronic control theory. However, in five- and seven-membered-ring amidines considerable lactam (50%) was produced. Their results suggest that the stereoelectronic control does not operate very well, if at all, in the five- and seven-membered-ring amidines and that a stereoelectronically favorable app lone-pair interaction only provides <2 kcal/mol lowering of the energy of activation. As pointed out by these authors, it is possible that the lone pairs on the –O$^-$ provide a much stronger driving force for expulsion of the leaving group than the app nitrogen lone pair. Indeed, Deslongchamps pointed out a "leveling" effect where each additional lone-pair interaction is less effective in controlling the breakdown of these tetrahedral species.[1,2]
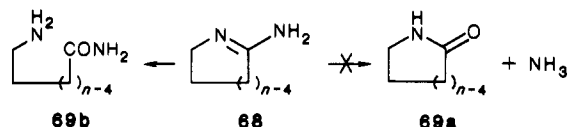
C. Stereoelectronic Effects In Reactions of Phosphate Esters

1. Hydrolysis of Six-Membered-Ring Phosphorus Heterocycles

As shown in Table I, the difference in the free energy of activation for the hydroxide-catalyzed hydrolysis for the epimeric pairs 11–15 only varies from 0.75 to 1.47 kcal/mol at 70 °C in 30% dioxane.[37,96] The chair equatorial b isomers thus always reacts *faster* by a factor of 3–9 (22 for 14b at 30 °C) than the chair axial a epimers. By comparing the equilibrium values ($\Delta\Delta G_0$ in Table I) with the difference in free energies of activation between the b and a epimers ($\Delta\Delta G^{\ddagger}$ in Table I), the faster hydrolysis for the b isomers can be entirely explained by ground-state destabilization.[37,96] In fact as shown in Figure 5, the difference in the transition-state energies for the hydrolysis of the 2,4-dinitrophenyl ester epimers is less than 0.2 kcal/mol. This suggests that both epimers of 14 have similar transition-state geometries: likely a half-chair, diequatorial ring trigonal bipyramid 70. As discussed earlier, ab initio molecular
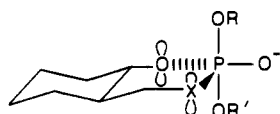
70: R,R' = H, Ar ; X = O, NH

orbital calculations (section IIIC) suggested that the magnitude of the rate acceleration expected from any stereoelectronic effect will depend upon whether the lone pairs are app to the translating bond in the rate-determining step. If nucleophilic attack is rate determining, then the optimal stereoelectronic conformation for facilitating bond making is quite different from that facilitating bond breaking. The lone pairs must be app to the leaving group in the bond-breaking step but app to the attacking group in the bond-making step. The attractiveness of transition-state **70** is that this problem is eliminated, since the lone pairs nicely overlap with both groups.

As in the hydrolysis of cyclic pyranosides, conformational flexibility prevents a direct measure of the stereoelectronic barrier EC* shown in Figure 4. This does not mean that stereoelectronic effects are not operative in these systems but simply that more constrained ring systems must be suitably designed.

2. Hydrolysis of Bicyclic and Acyclic Phosphates and Phosphorothionates

The rate of hydrolysis of the bicyclic phosphate **71** is 5.2 × 10³ times that of the acyclic phosphate **73** while the rate of hydrolysis of the bicyclic phosphorothionate **72** is 8.1 × 10² times that of the acyclic phosphorothionate **74**.[97] As can be seen from structure **75**, each

71

$(EtO)_3P{=}O \xrightarrow{\text{0.6 M NaOH}} (EtO)_2PO_2^- + EtOH$

73

72

$(EtO)_3P{=}S \xrightarrow{\text{0.6 M NaOH}} (EtO)_2POS^- + EtOH$

74
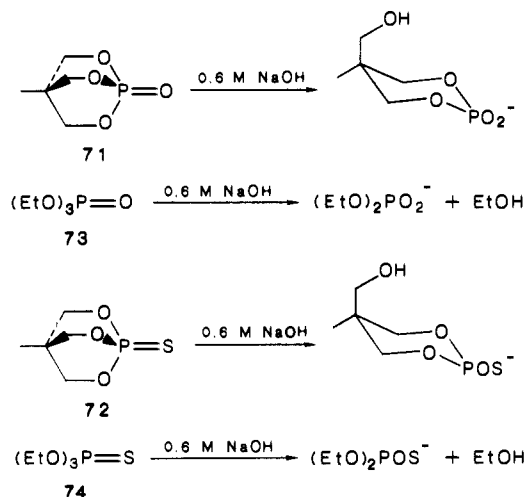
of the two equatorial endocyclic oxygens have lone electron pairs approximately app to the breaking apical P–O bond. This is suggested to be mainly responsible for the increased rate of cleavage of this bond relative to its acyclic analogue triethyl phosphate or phosphorothionate. In the acyclic compounds triethyl phosphate and phosphorothionate freezing of one conformation is required to put two lone pairs app to the breaking P–O bond, **76**. This conformational restric-

75 **76**

SCHEME VI

77 **78** **79**

80 **81** **82**
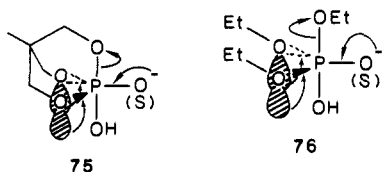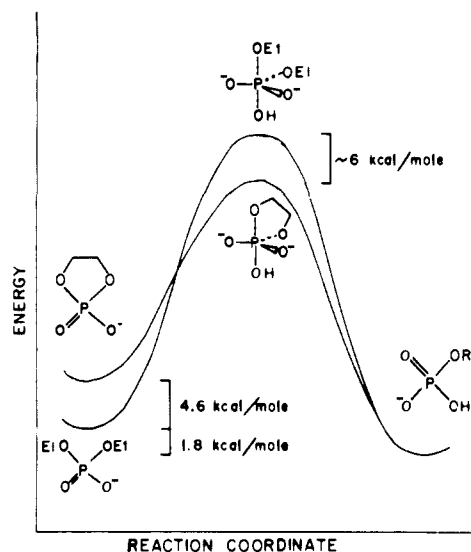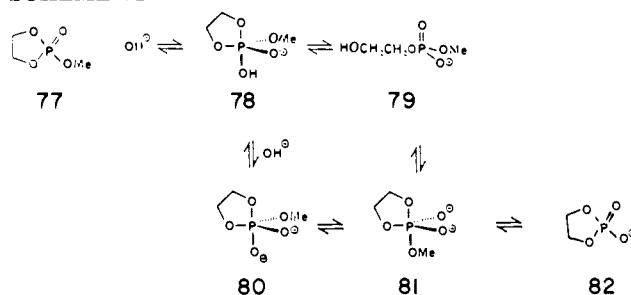
Figure 6. Reaction profiles for ⁻OH-catalyzed hydrolysis of diethyl phosphate and ethylene phosphate (**82**). Figure taken with permission from Gerlt et al.[103] Copyright Journal of Biological Chemistry 1975.

tion will be entropically disfavored.[17,18,19] These results suggest that the reactivity difference between bicyclic esters and their acyclic counterparts can be accounted for by stereoelectronic effects in the transition states/intermediates, although other factors such as ring strain remain to be considered as well.

3. Hydrolysis of Ethyl and Methyl Ethylene Phosphates

The rate of hydrolysis of five-membered-ring phosphates such as methyl ethylene phosphate (MEP) (**77**) and ethylene phosphate (EP) (**82**) (Scheme VI) is 10⁶–10⁸ times faster than that of their acyclic analogues, respectively. Westheimer and co-workers[98–102] proposed that this rate acceleration was due to the energy released in going from a strained cyclic ester to a "strain-free" cyclic phosphorane transition state. However, as pointed out by Gerlt, Westheimer, and Sturtevant,[103] and shown in Figure 6, the amount of ring strain (4–6 kcal/mol) is insufficient to explain the total 10–11 kcal/mol lowering of the activation energy of the five-membered ring phosphates relative to their acyclic analogues.

As discussed in section IIIC, the molecular orbital calculations suggest that the stereoelectronic effect could significantly facilitate endocyclic P–O ester bond cleavage and that proper orbital overlap could be responsible for the unexplained ~6 kcal/mol stabilization[103] of the cyclic phosphorane transition state compared to the acyclic transition state[17–19] (Figure 6). In **81**, the two lone pairs on the sp³-hybridized basal ring

SCHEME VII

77   79   82   83
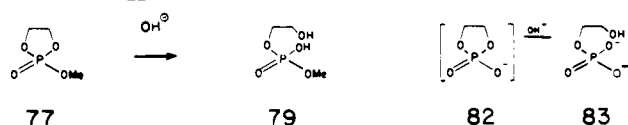
ester oxygen are oriented anticlinal (dihedral angle 120°) relative to the apical ring ester bond, or if viewed in terms of an sp^2-hybridized oxygen, the single sp^2-hybridized lone pair is oriented app to the apical ring ester bond). Note that the endocyclic cleavage transition state of 81 resembles 29 in Figure 3, which is 11 kcal/mol lower energy than 30 which corresponds to the exocyclic cleavage transition state. Indeed as we argued in section IIIC (hydrolysis of six-membered-ring vs. acyclic phosphates), in the five-membered-ring esters the ring constrains the lone pairs in a stereoelectronically favorable orientation while in the acyclic transition state proper app lone pair overlap would require "freezing" of one or more rotational degrees of freedom about the ester bonds.[8] It is thus significant that a considerable portion of the rate difference between cyclic and acyclic reactions is entropically driven. It could be argued that a stereoelectronic effect on the rate of reaction should only be possible if ring ester bond cleavage in the pentacovalent intermediate and not addition of hydroxide is rate limiting. However, the rate-determining step in the reaction is not known, and lone-pair mixing into the *elongated* endocyclic bond in the pentacovalent transition state for the addition step should also be more favorable than into the same bond in the ground state (see section IIID).

A major difficulty with the stereoelectronic effect explanation for a portion of the rate acceleration was the observation of significant exocyclic cleavage in the product-determining step of the reaction.[98,99] As shown in Schemes VI and VII, hydrolysis of 77 (MEP) yielded not only the expected product of stereoelectronic control, the endocyclic cleavage product, methyl 2-hydroxyethyl phosphate (79), but as much as 1–50% of an exocyclic product, 2-hydroxyethyl phosphate (83), formed by rapid hydrolysis of the initially formed ethylene phosphate 82. Based on GC and proton NMR analysis, very small amounts (1% or less) of the exocyclic cleavage product 82 were reported at dilute hydroxide concentration (pH 10–13). However, at higher hydroxide concentrations, 5 and 10 M, 9% and 15% of exocyclic cleavage were observed, respectively.

The increased exocyclic cleavage of MEP (77) in strong alkali was explained in terms of a mechanism (Scheme VI) involving initial formation of a trigonal-bipyramid, pentacoordinate intermediate,[99] which after proton removal yields the dianionic intermediate 80. Rapid pseudorotation of 80 yields 81, which in turn breaks down to give the exocyclic cleavage product 82 (ethylene phosphate, EP). The pK_a of the apical hydroxyl group of the monoanionic phosphorane intermediate was estimated to be greater than 13 and formation of the dianionic phosphorane, in very strong alkali, would place the oxyanion in an unfavorable apical position, thereby increasing the rate of pseudorotation to 78.[98] Knowles and co-workers[104] showed that the substitution reaction indeed leads to retention of configuration, consistent with the overall mechanistic scheme. Thus, increased hydroxide concentration

would increase the percentage of exocyclic cleavage.

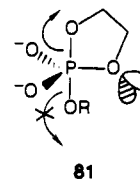An important controversy in the recent literature developed over results and interpretation of the product distribution in the strong alkaline region.[105,106] As argued above, according to the stereoelectronic effect,[14,17,18,67] intermediate 81 is highly favored for en-

81

docyclic cleavage: note the basal oxygen lone pairs of the ring-constrained pentacovalent transition state are app *only to the apical endocyclic ester bond and not to the exocyclic bond.* Therefore, we should expect very little exocyclic cleavage product even at very high concentrations of NaOH. In our laboratory, Taira et al.[65,66] carried out the hydrolysis of MEP (77) *at low concentration* of ester in 5 M NaOH with a rapid-quench method and analyzed the reaction products by phosphorus NMR instead of the earlier proton NMR and GC methodology. Our laboratory found that, compared with Kluger et al.'s earlier results,[99] there is much less (0 ± 3% vs. the reported 4–15%) exocyclic cleavage product produced in the strong-base-catalyzed hydrolysis of MEP. These results were consistent with the prediction of the stereoelectronic theory.[14,17,18]

However, recently Kluger and Thatcher[105,106] rechecked Kluger et al.'s earlier results[99] by proton (and to a lesser extent ^{31}P) NMR. By monitoring the appearance of the methanol peak, they found that under strong alkaline condition the fraction of "methanol" (which they equate with the exocyclic cleavage product) in fact appears to increase to as much as 24% exocyclic cleavage in saturated NaOH (18.5 M) and (9.2% exocyclic cleavage even in 5.6 M NaOH). It is very important to note that Kluger et al.'s earlier study and our studies[65–67,107] were largely done at *low concentrations of MEP* (<0.02 M). Kluger and Thatcher's reinvestigation[106] was done at much higher concentrations (0.3–0.9 M) MEP although more recently[105] two lower concentration runs were described. In order to resolve the discrepancy between these reports our laboratory has repeated our own earlier work as well as followed the experimental protocol of Kluger and Thatcher at various MEP concentrations.[107]

In all cases we have only seen 2–4% exocyclic cleavage in the strong-base-catalyzed hydrolysis of MEP.[107] In contrast to Kluger and Thatcher's result, this ratio does *not* change greatly with base concentration even when the reaction is not run under dilute conditions. In the case of ethyl ethylene phosphate the percentage of exocyclic cleavage product is even lower (≪2%).

Most importantly we interpret our experimental data as suggesting that the large increase in percent exocyclic cleavage (to as much as 24%) claimed by Kluger and Thatcher is due to an artifactual dimerization reaction that occurs at the high concentration of MEP used in their study (Scheme VIII).[107]

Proposed Resolution of Differences between Various Groups. As indicated in Scheme VIII, at higher concentrations of MEP, a "dimer" is formed by the reaction of the endocyclic cleavage product MHEP

SCHEME VIII
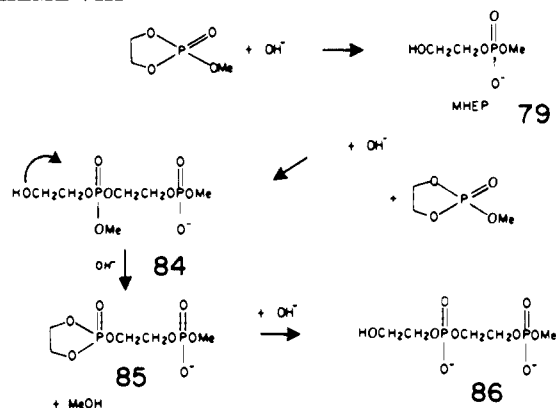
(77) and unreacted MEP. This "dimer", [[[(hydroxy-ethyl)oxy]methoxyphosphinyl]oxy]ethyl methyl phosphate (84) contains one diester phosphoryl group and one triester phosphoryl group. The diester phosphoryl group hydrolyzes very slowly, which would be similar to that of MHEP (79) in alkaline solution.[65] However, for the triester phosphoryl part with the β-hydroxy group, the hydrolysis rate will be significantly enhanced due to an anchimeric acceleration.[65,108] Thus, triester 87 with a β-hydroxy group hydrolyzes very fast in base with a half-life of 9 min at pH 9.[65,108]
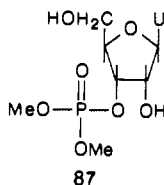
In the alkaline hydrolysis of MEP, the initial triester dimer 84 would thus have a very short lifetime. With anchimeric assistance from the β-hydroxy group, it will cyclize to *generate methanol* and cyclic triester dimer 85 (Scheme VIII). Further rapid hydrolysis of 85 finally yields phosphodiester dimer 86. It is this second form of the dimer ("diester dimer" 86) that Kluger and Thatcher presumably also observe in their study. Kluger and Thatcher, however, proposed a mechanism for this dimer formation in which EP (82) the initial hydrolysis product of MEP, reacts with the endocyclic cleavage product MHEP (79) to form the [[(hydroxy-ethyl)phosphono]oxy]ethyl methyl phosphate (HEMPP, 86). We disfavor this mechanism for two reasons: First, a neutral phosphate triester such as MEP is much more reactive than the monoanionic diester EP (82) especially with an anionic nucleophile. Second, during most of the reaction, the concentration of MEP is much higher than EP. Our laboratory has also obtained ^{31}P NMR spectra in support of the dimer structures 84 and 86, consistent with the mechanism for their formation shown in Scheme VIII.

Thus, because dimer is indeed also produced from the reaction between MEP and MHEP (79), methanol can thus be generated by an additional route other than through the exocyclic cleavage of MEP, i.e. hydrolysis of the "triester dimer" 84. Kluger and Thatcher monitor percent exocyclic cleavage by integration of the methanol peak in the ^{1}H NMR spectrum, and this method of product analysis is therefore potentially subject to serious error. Disregarding the artifactual production of methanol from the dimerization reaction,
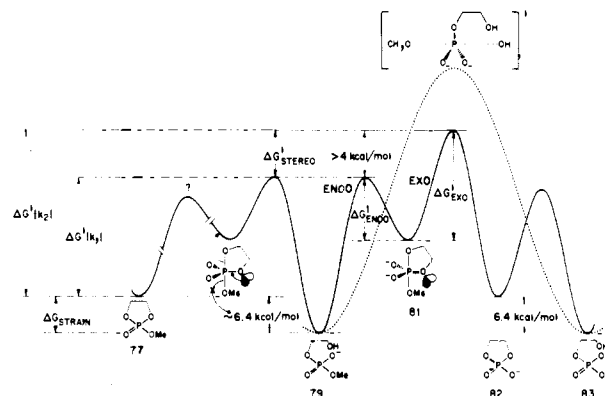
Figure 7. Reaction profiles for base-catalyzed hydrolysis of methyl ethylene phosphate (77) and methyl 1-hydroxyethyl phosphate (79). Derived from Taira et al.[66]

SCHEME IX
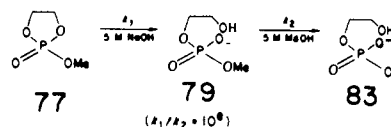
in contrast to the claims of Kluger and Thatcher there is little if any increase in exocyclic cleavage with base. However, analysis based upon our more recent ^{31}P NMR data does possibly show $\sim 3 \pm 1.5\%$ (S/N ratio ~ 60) of exocyclic cleavage product for MEP hydrolyzed in 1–9 M NaOH.[107] Still, an initial report from our laboratory[65,66] of $0 \pm 3\%$ at low MEP concentration (in dioxane) indeed was and still is correct within the signal-to-noise (S/N 30) of the early spectra and the reported accuracy of the measurement. Actually even this $3 \pm 1.5\%$ exocyclic cleavage is very difficult to establish with current methodology. Thus, if the hydrolysis is conducted at the concentrations reported in our initial report[65-67] (0.017 M MEP, added as a dilute solution of MEP in dioxane), the apparent amounts of exocyclic cleavage and dimer products are even less ($\sim 1\%$). This suggests that local high concentrations of MEP resulting from addition of neat MEP in Kluger and Thatcher's method[105,106] could be responsible for the increased amount of dimer and exocyclic cleavage product. (Note in neutral or acidic solution, 10–50% exocyclic cleavage is observed[99]–addition of neat MEP to dilute base with subsequent rapid hydrolysis and acid production could neutralize the base and generate regions of very low basicity.)

Determination of the Magnitude of the Stereoelectronic Effect from Kinetic and Thermodynamic Parameters. From ^{18}O-labeling studies and previous data in the literature, we have shown that the pathway for the formation of 79 is 77 → 78 → 80 → 81 → 79 (Scheme VI; Figure 7). Further, the pathway for the formation of 83 from 79 is 79 → 81 → 82 → 83 as schematically shown in Figure 7. The observed rate constant[66] (k_2) for the formation of 83 via 81 from 79 in 5 M NaOH is ca. 5×10^{-4} min^{-1}. An extrapolation from Kluger et al.'s pH vs. rate profile[99] suggests that the rate constant for the formation of 79 from 77 via 81 is at least 5×10^4 min^{-1} in 5 M NaOH. Therefore, the strained cyclic five-membered-ring phosphate triester 77 reacts at least 10^8-fold faster than its strain-free initial diester product 79 via the common intermediate 81. This factor of 10^8 corresponds to a 11 kcal/mol

difference in activation free energies[65] (Scheme IX). Since both endocyclic and exocyclic products must be formed through the same transition state/intermediate **81**, it is possible to estimate the magnitude of the stereoelectronic effect. Since, as discussed earlier in this section, only the endocyclic cleavage product is stereoelectronically assisted by the endocyclic basal oxygen lone pairs and the lone pairs on the other two basal oxygens can equally assist both endocyclic and exocyclic cleavage, the endo/exo activation energy difference from the intermediate **81** reflects the stereoelectronic effect due to the endocyclic basal oxygen lone pairs. From Figure 7

$$\Delta G^{\ddagger}_{stereo} = \Delta G^{\ddagger}_{exo} - \Delta G^{\ddagger}_{endo} =$$
$$\Delta G^{\ddagger}(k_2) - \Delta G^{\ddagger}(k_1) - \Delta G^{\ddagger}_{strain} \quad (5)$$

where $\Delta G^{\ddagger}_{stereo}$ is the activation energy difference due to the stereoelectronic effect. Since k_1/k_2 is at least 10^8, $[\Delta G^{\ddagger}(k_2) - \Delta G^{\ddagger}(k_1)]$ is at least 11 kcal/mol. Although the strain in methyl ethylene phosphate (**77**) is not yet certain, the strain in the monocyclic five-membered ring phosphodiester **82** with respect to its hydrolysis product **83** is reported[103] to be 6.4 kcal/mol. If it is assumed that the strain in **77** with respect to **79** is equal to that of **82** with respect to **83**, $\Delta G^{\ddagger}_{stereo}$ can be estimated from eq 10 to be ~4.6 kcal/mol. Thus, the rate of partitioning of **81** must favor the endocyclic path by 4.6 kcal/mol over the exocyclic path, although a portion of this difference is also attributable to an increase in ring strain in forming the strained ethylene phosphate (**82**) in the exocyclic cleavage path. The transition state, however, will be closer in structure to the high-energy trigonal-bipyramidal pentacovalent intermediate **81**, which is expected to have little bond angle strain.[98,99,101,102] Thus, this 4.6 kcal/mol difference in activation free energies arises at least in part from the stereoelectronic effect.

Comparison of Methods To Estimate the Stereoelectronic Effect. From the kinetic and thermodynamic parameters we have been able to estimate the magnitude of the stereoelectronic effect in this system. Since this has been estimated to be up to 4.6 kcal/mol, we should detect very little exocyclic cleavage in the alkaline hydrolysis of **77**. If, as reported earlier, 11% of exocyclic cleavage[99] occurs in 5 M NaOH, the stereoelectronic effect contributes only a small portion (1.3 kcal/mol) of the kinetically estimated value of 4.6 kcal/mol.

However, in spite of the claims of Kluger and Thatcher,[105,106] we believe that the alkaline hydrolysis of MEP has *at most* 3 ± 1.5% exocyclic cleavage in strong base, which corresponds to about 2 kcal/mol in lowering the activation energy of the transition states between exocyclic and endocyclic cleavage. Because the pK[109] of ethanol ($pK = 15.9$) is greater than that of methanol ($pK = 15.4$), exocyclic cleavage of the better leaving group could be favored by 0.4 kcal/mol. Thus, the minimum stereoelectronic effect for cleavage of comparable leaving groups may well be at least 2.5 kcal/mol, consistent with the kinetic arguments presented in the previous section that suggest a stereoelectronic effect of up to 4.6 kcal/mol. Most significantly, our laboratory has also reinvestigated[107] the amount of exocyclic cleavage in ethyl ethylene phosphate, and even at high concentration of the cyclic

phosphate in 1–5 M NaOH <0.2% exocyclic cleavage is observed.

Contrary to Kluger and Thatcher's claims,[106] we never suggested that the stereoelectronic effect "requires intermediate **81** to react exclusively to give endocyclic cleavage". We clearly indicated that the stereoelectronic effect could be responsible for as much as 10^3–10^5 rate acceleration.[66] What *would* invalidate our argument, however, is a large increase in the percent exocyclic cleavage with increasing base. Since we believe that this increase (to as much as 24% as claimed by Kluger and Thatcher) is due to an artificial dimerization reaction, the stereoelectronic effect continues as a quite viable explanation for a significant portion of the rate acceleration in five-membered-ring phosphate esters.

4. Estimation of the Contributions of Ring Strain and the Stereoelectronic Effect in Five-Membered-Ring Phosphate Esters

In contrast to the cyclic five-membered-ring phosphate esters that hydrolyze 10^6–10^8 times faster than their acyclic analogues, a five-membered-ring cyclic phosphinate ester **89** hydrolyzes in base only 6.2×10^3 faster than its corresponding acyclic analogue.[110] Our laboratory utilized the difference in rate of hydrolysis of esters **88** and **89** to attempt to separate the contributions of ring strain and stereoelectronic effects.
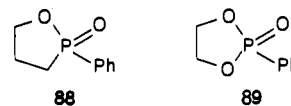
Estimation of Ring Strain Contribution to Rate Acceleration. As discussed in the previous section, the measured enthalpies of hydrolysis of ethylene phosphate and diethyl phosphate, as indicated by Gerlt et al.,[103] are 6.4 and 1.8 kcal/mol, respectively (Figure 6). The difference in the enthalpic energy is thus only 4.6 kcal/mol of strain in the cyclic five-membered-ring phosphodiesters. Unfortunately sufficiently accurate thermochemical measurements of ring strain in five-membered-ring phosphate triesters are unavailable. In methyl ethylene phosphate, reported enthalpic strain varies between 7 to 9 kcal/mol in an earlier report[111,112] and 5.5 kcal/mol[113] for a later report. Even in the ethylene phosphate diester five-membered-ring system the 4.6 kcal/mol of ring strain is insufficient to explain the total 10^8-fold rate acceleration relative to its acyclic analogue (corresponding to an activation energy difference of 10–11 kcal/mol).[103] As described in the previous section, we suggested that much of the 6 kcal/mol difference in energies of the acyclic vs. cyclic transition states could be attriuted to a stereoelectronic effect.[14,17,18] In the triester five-membered-ring system, the situation is not as clear. Methyl ethylene phosphate hydrolyzes 10^6 (from ref 99) and ethyl ethylene phosphate 2×10^7 (from ref 114) times faster than their acyclic analogues, corresponding to 8.3–10 kcal/mol difference in activation energies. Because estimated ring strain is as high as 9 kcal/mol, it could be responsible for essentially all of the rate enhancement for hydrolysis of methyl or ethyl ethylene phosphate. If this is the case, a stereoelectronic effect would not need to be invoked in order to explain the rate acceleration. However, in the previous section I have estimated that the stereoelectronic effect could well contribute 3.2–4.6

SCHEME X
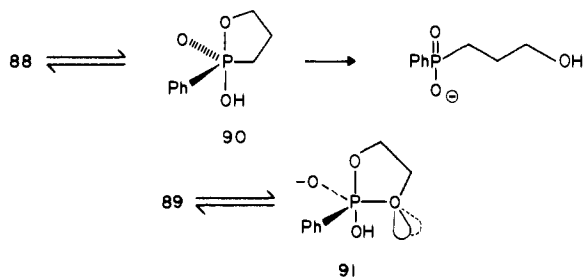
kcal/mol stabilization of the cyclic transition state. This would suggest that release of ring strain accounts for the remaining 5–6 kcal/mol difference in activation energies in the cyclic vs. acyclic systems. Hydrolysis of 88 and 89 in base, however, potentially provides a good test for the relative importance of ring strain and the stereoelectronic effect contributions to the rate accelerations in these systems. As shown in Scheme X, both 88 and 89 will presumably form phosphorane intermediates 90 and 91, respectively. However, there are no basal ring oxygen lone pairs in 90 to participate in a stereoelectronic effect aiding in the expulsion of the leaving group. The rate difference in the base-catalyzed hydrolysis between 88 and and its acyclic analogue ethyl ethylphenylphosphinate (92) thus could provide a good
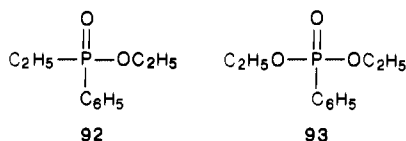
estimate for ring-strain effects alone. Hydrolysis of 89 will presumably reflect both ring strain and the stereoelectronic effect. Significantly, the difference in rate between 88 and 92 is 6.2×10^3, corresponding to an activation free energy difference of 5.2 kcal/mol. This is comparable to the reported ring strain value, 5.5 kcal/mol, obtained from a measurement of the heat of hydrolysis of methyl ethylene phosphate by Kaiser et al.[113] It is also comparable to the ring-strain estimate in ethylene phosphate.[103]

Estimation of Stereoelectronic Effect. With a more confident value, 5.2 kcal/mol, of ring strain in hand,[110] one can estimate the contribution of the stereoelectronic effect to the rate acceleration in five-membered ring phosphate esters. The rate difference in base hydrolysis between 89 and its acyclic analogue diethyl phenylphosphonate (93) is 1.48×10^6, which corresponds to a difference in free energy of activation of 8.4 kcal/mol.[110] This is a comparable rate acceleration to that of MEP (77) and suggests that the phenyl ring does not contribute any unusual steric energy to the system. Assuming ring strain in dioxa- (89) and oxaphospholane (88) is nearly the same, the ring strain effect in 88 of 5.2 kcal/mol can be subtracted from the difference in free energy of activation between 89 and 93, leaving a value of 3.2 kcal/mol. We have suggested that the stereoelectronic effect is responsible for this 3.2 kcal/mol difference.[110]

The one remaining complication in this analysis that cannot be entirely discounted is the possibility that eclipsing interaction differences casts in doubt the assumption that ring strain effects in 88 and 89 are comparable. It is certainly possible that eclipsing interac-

tions in PCH_2CH_2- are greater in the cyclic transition state for hydrolysis of 88 than in the acyclic transition state for hydrolysis of 92. However, ethyl propylphostonate (94) hydrolyzes in base 3×10^5 times faster
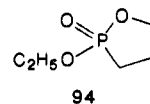

than its acyclic analogue.[114] Because this is comparable to the rate acceleration in MEP, 77 (10^6), ethyl ethylene phosphate (2×10^7), and 89 (1.5×10^6), eclipsing interactions resulting from substitution of the ring oxygen by a methylene appear to be minor. In fact, it is rather surprising that the rate acceleration for hydrolysis of the phostonate is nearly as great as that of MEP if our arguments about the significance of the stereoelectronic effect are correct. Obviously, as in 88, phostonate 94 does not have an app lone pair on a ring atom to stereoelectronically aid in expulsion of the endocyclic P–O ester bond (the phostonate proceeds with complete endocyclic cleavage in keeping with the pseudorotation rules of Westheimer[98]). An important difference between phosphinate 88 and phostonate 94 is the potential availability of an electron lone pair on the exocyclic alkoxyl oxygen in the latter. In the transition state 95
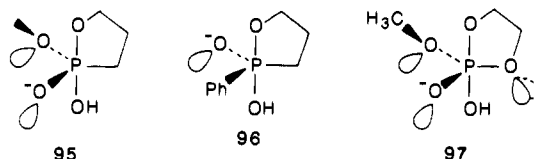
for cleavage of the endocyclic ester bond in the hydrolysis of 94, two lone pairs in 95 can be oriented app to the apical P–O bond, while in 96 there is only one lone pair on the basal oxyanion to stereoelectronically assist in cleavage of the apical bond. As demonstrated by Deslongchamps,[1,2] there appears to be a leveling effect on the magnitude of the stereoelectronic acceleration afforded by increasing numbers of app lone pairs. Two lone pairs will likely be nearly as effective as three, and thus in the transition state 81 for hydrolysis of methyl ethylene phosphate, the third lone pair may be unnecessary. This could explain why phostonate 94 and methyl ethylene phosphate hydrolyze 3×10^5 and 10^6 times faster than their acyclic analogues, respectively, while cyclic phosphinate 88 hydrolyzes only 6.2×10^3 times faster than its acyclic analogue. Note that the $k_{cyclic}/k_{acyclic}$ rate ratio for ethyl ethylene phosphate is 70 times larger than the rate ratio for ethyl propylphostonate.[114] This could be a reflection of eclipsing interaction differences or a real measure of a stereoelectronic effect. This analysis, of course, is entirely speculative, and it is not very profitable to push it much further.

Conclusion. Thus, we believe it is possible to separate the effect of ring strain and the stereoelectronic effect in the hydrolysis of cyclic five-membered-ring phosphorus esters. The magnitude of the ring strain effect is likely to be in the range 4–6 kcal/mol for related cyclic five-membered rings. There may well be a ca. 3 kcal/mol stereoelectronic effect in the cyclic five-membered-ring phosphorus ester systems.

In conclusion, the search for support of the stereoelectronic effect at phosphorus has often been frustrated

by conformational flexibility of the reactants.[37,58,97,115] In this section we found rate differentials in reactions of cyclic and bicyclic phosphate esters that provide evidence in support of the stereoelectronic effect. In each of the reactions discussed, alternative explanations for these kinetic effects may be offered (and indeed could be partially correct!). However, it is in this *growing body* of evidence that we continue to find strong support for the stereoelectronic effect.

V. Stereoelectronic Effects in Enzymatic Reactions

A. Estimation of the Catalytic Advantage in Stereoelectronic Control of Enzymatic Reactions

In previous sections, we noted that in suitably constrained systems the stereoelectronic effect can be responsible for significant rate accelerations. Presumably, one of the important aspects of enzymic catalysis is to constrain substrates into optimal conformations.[1-4,18,116,117] In this section we will consider the evidence that enzymes indeed take advantage of proper orbital overlap and that the stereoelectronic effect makes an important contribution to a wide range of enzyme-catalyzed biochemical transformations.

It is important to point out that the potential enzymatic activation energy lowering by stereoelectronic effects is not simply limited to ground-state *enthalpy* differences between different conformers.[18] Thus, if a given conformation (such as the g,t conformation of Figures 2 and 3) is the stereoelectronically optimal conformation for reaction, based upon enthalpy considerations alone, the enzyme-bound g,t conformational isomer should only react faster than the nonenzyme-bound, conformationally flexible molecule by a factor representing the energy difference between the lowest energy conformation and the stereoelectronically optimal g,t conformation. The basis for this statement derives from the following argument. Assuming again that the g,t conformation is significantly more reactive than the other conformations, then only the fraction of the total freely interconverting molecules possessing this g,t conformation is reacting in solution. This Boltzmann distribution fraction will be determined by the ground-state energy difference between the reactive g,t and less reactive conformations. Any further stereoelectronic acceleration of the enzymatic reaction can only be achieved by increasing the fraction of the reactive conformation. However, as shown in the previous sections, the ground-state stereoelectronic (anomeric) effect is often quite modest (1–2 kcal/mol). Thus, in solution the fraction of the stereoelectronically reactive conformation is already quite high, and it would appear that the enzyme cannot take much further catalytic advantage of the stereoelectronic effect. As we will discuss in a later section, for some enzymes (as for example possibly lysozyme) that distort the substrate into unusual high-energy conformations that provide for optimal orbital overlap, the enthalpic contribution to catalysis may still be substantial.

The actual stereoelectronic advantage in reacting via a stereoelectronically optimal conformation (such as the g,t conformation) is likely to be much larger than indicated by these enthalpic arguments. We have ignored entropic considerations, and any stereoelectronic effect

may well be masked by the rather substantial *unfavorable* entropic effects. Assuming again that only a select group of conformations is stereoelectronically reactive, then during the course of the reaction various rotational degrees of freedom must be lost. The rate of the nonenzymatic reaction will reflect this internal entropic disadvantage, which may be as large as 8 eu (2.4 kcal/mol at 25 °C) per lost degree of freedom.[116] For freezing 2 rotational degrees of freedom, this entropic factor may represent a rate difference of up to 10^3–10^4. In order for the nonenzymatic reaction to be stereoelectronically controlled, the enthalpic, stereoelectronic advantage must be large enough to at the very least cancel the 4–5 kcal/mol entropic disadvantage of freezing 2 rotational degrees of freedom. We have seen how this conformational flexibility can readily mask the stereoelectronic effect in the reactions of acetals (section IVA) and phosphate esters (section IVC). Presumably an enzyme, however, can utilize intrinsic binding energy[116] to restrict the substrate into the stereoelectronically reactive conformation. Hence, the full stereoelectronic enthalpic gain is realized without any entropic loss.

It is significant that our best estimate at the present time for this enthalpic kinetic stereoelectronic effect in five-membered cyclic phosphate esters relative to simple acyclic esters is indeed ca. 3–5 kcal/mol (or rate accelerations of 10^2–10^4). The observed 12–18-eu less favorable entropy of activation for acyclic vs. cyclic phosphate esters[114] may well arise from the immobilization of the freely rotating ester bonds.

As we will see, it is quite possible that enzymes take advantage of the potential stereoelectronic *catalysis* and *specificity* by binding substrates into proper conformations. It is important to emphasize that enzymic catalysis very much derives from the enzyme's special capacity to stabilize (and hence lower the energy of) the transition state of the reaction.[116,118-120] However, for most enzymatic reactions there is probably no *one* unique transition state. Thus, as Albery and Knowles[121] argued, in the "evolutionary perfection" of an enzyme catalyst in facilitating a multistep reaction, eventually the enzyme must confront the problem of finding a mechanism that lowers the barrier to each elementary step. Lowering the barrier to the rate-determining step will accelerate the reaction, but then any further lowering will not result in any further catalysis since another elementary step will become rate limiting. In order for an enzyme to achieve further catalytic efficiency, it must now evolve new or better mechanisms to lower the new rate-determining step barrier until this step also no longer becomes rate limiting. Evolutionary pressure will thus result in an enzyme-catalyzed reaction in which all of the barriers are of approximately equal height, as well as all of the bound intermediates are of equal free energy. No one step is rate limiting, and, in fact, data support this view.[121]

These arguments thus suggest that an enzyme cannot simply function by locking a substrate into a *single* stereoelectronically kinetically favorable conformation. If, as we will see, a different conformation is required for stereoelectronic acceleration of different steps in a reaction, then an enzyme must be sufficiently conformationally flexible at its active site to stabilize each and every one of these partially rate-determining transition

SCHEME XI. Proposal of Stereoelectronic Control in Secondary Amide Hydrolysis by α-Chymotrypsin[147]
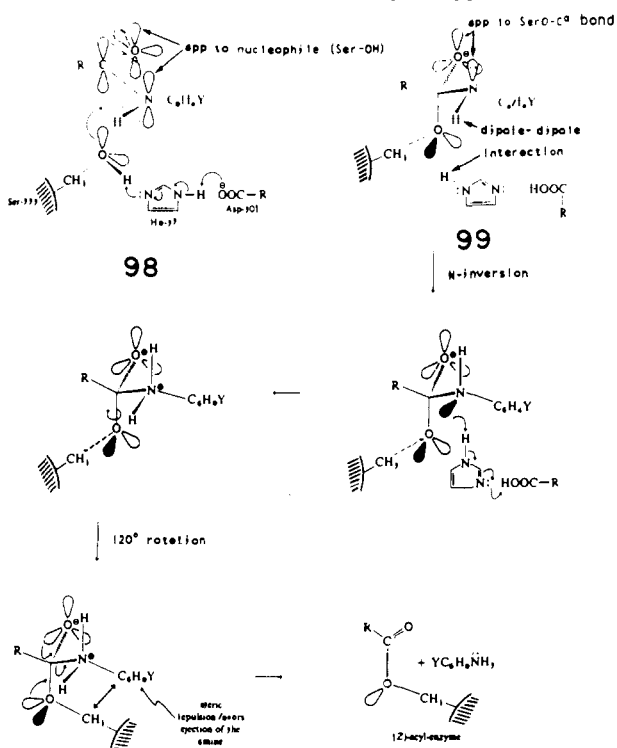
states. Such multiplicity of conformational states for enzymes has indeed been observed, especially in NMR[122] and fast-kinetic, relaxation spectra of enzymes and enzyme complexes.[123]

B. Serine Proteases

Several papers addressed the importance of stereoelectronic effects in the mechanism of action of the serine proteases, such as α-chymotrypsin.[7,10,13,62-64,124,125] Chymotrypsin and likely all other serine proteases proceed via an acylenzyme intermediate in which formation of the acylenzyme intermediate and hydrolysis of the intermediate in turn proceed via tetrahedral intermediates (Figure 8; Scheme XI). Concentrating only on the reaction path between Michaelis complex **98** and acylenzyme **101**, the enzyme must catalyze formation and breakdown of the tetrahedral intermediates **99/100** in a minimum two-step reaction. If chymotrypsin is "perfected," then each of these steps is partially rate limiting. Kinetic evidence supports the existence of this tetrahedral intermediate.[126-128] The enzyme must thus stabilize *both* transition states in the formation and breakdown of the tetrahedral intermediate. Thus, as argued in the previous section, if stereoelectronic effects operate for one transition state, they will likely operate for both. The optimal stereoelectronic conformation for formation of the tetrahedral intermediate must, as argued below, be different from the optimal stereoelectronic conformation for breakdown of the intermediate. Passage from one transition state to the other will require single-bond rotation about C–O and C–N in the tetrahedral intermediate. Our laboratory has argued that a most important function of the enzyme is to provide for these conformational changes in the tetrahedral intermediate complex.[13,62]

Maximization of both the normal and counterbalancing (see section IIIC) stereoelectronic effects sug-
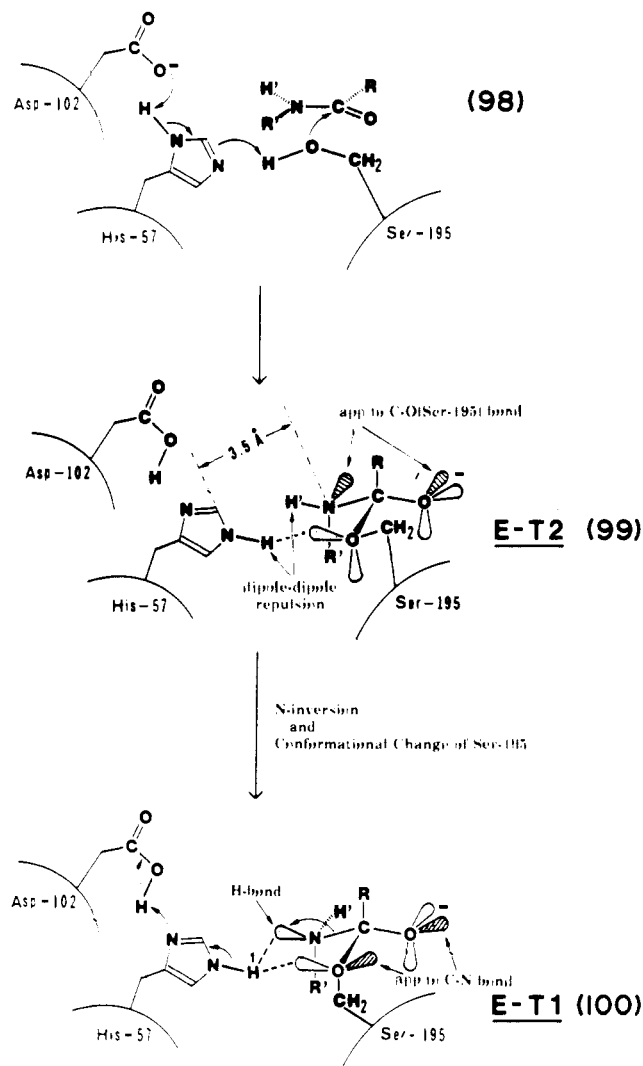
Figure 8. Schematic drawing of steps in acylation reaction of α-chymotrypsin partially derived from ref 147. Antiperiplanar lone pairs to the scissile bond are shaded. Reproduced with permission from ref 62.

gests, as discussed in the theory section IIIB and detailed in Figure 2, that in acyl addition/elimination reactions where both bond making in the addition step and bond breaking in the elimination step are partially rate limiting, *rotation about the scissile bonds during the reaction is essential*.[13] The best stereoelectronic (and counterbalancing stereoelectronic) lone-pair orientation on N and O for C–N bond making is going to be the wrong orientation for optimal stereoelectronic (and counterbalancing) stereoelectronic interactions for C–O bond breaking.

Thus, for C–N bond formation in Figures 2 and 8, stereoelectronically the lone pair on the adjacent oxygen must be app to the translating (scissile) C–N bond and no lone pair on the N should be app to the adjacent C–O bonds. This is achieved in the t,g conformation of transition state **20** (these are approximate torsional angles for the C–N and C–O₂ bonds respectively, with torsional angles defined in Figure 1 with $X_1 = N$, $X_2 = O_2$, and $Y = C$). However, for C–O bond breaking, the lone pair on the adjacent nitrogen must be app to the scissile C–O bond and no lone pair on the scissile bond oxygen should be app to the adjacent C–N bond. This is achieved in the g,t conformation of transition state **22**. Only with rotation about the C–N and C–O₂

bonds during the reaction can the stereoelectronic effect optimally lower the activation barrier for both steps and hence lower the overall activation barrier.

This rotation *during* reaction is not feasible for a concerted S_N2-type displacement reaction where the rotation rate will only be a fraction of the rate of translation across the top of the energy barrier.[129] While an app lone-pair effect could facilitate the first, largely attack phase of the reaction, the latter, largely displacement stage of a single-barrier pathway cannot be helped by the now cis lone pair. We expect therefore that the app lone-pair effect cannot play an important role in S_N2-type reactions. If, however, an intermediate, no matter how high its energy, exists along the reaction pathway, bond rotation is allowed and "stereoelectronic catalysis" of both bond making and breaking is possible. The intermediate need only have a lifetime of a single-bond rotation. Displacement reactions at tetrahedral carbon (S_N2 type) cannot be stereoelectronically catalyzed while those at tetrahedral phosphorus (and other second- and third-row elements) may well obey these principles since pentacovalent intermediates are realizable.

While stereoelectronic lone-pair effects should not be important for carbon S_N2 reactions, as discussed in section IV, they indeed appear to operate in reactions involving trigonal or tetrahedral centers such as acyl addition/elimination reactions. The tetrahedral intermediates in these reactions will generally have lifetimes long enough to permit single-bond rotation.

Blow[130] proposed a detailed stereochemical analysis for the steps in formation of the acyl enzyme that incorporates chemical modification, kinetic, and X-ray diffraction[131-137] data on a number of serine proteases and their complexes. As discussed in the following, Taira and Gorenstein[13,62] emphasized the additional stereochemical restrictions placed upon the mechanism resulting from the stereoelectronic requirements.

Shown in Figure 8 is a description of the catalytic events in the acylation reaction as presented by Blow[130] and modified[13,62] to incorporate these stereoelectronic requirements. Summarizing the overall scheme, in **98** (Figure 8) the trigonal amide substrate (bonds in black) binds to the substrate binding pocket and the carbonyl oxygen near the oxyanion hole, hydrogen bonding to the backbone N–H's of Ser[195] and Gly[193]. The leaving-group amide N' is near $N^{\epsilon 2}$ of His[57]. Crucial to our argument as discussed by Blow (and others)[130,138-141] is the conformational mobility about the $C^\alpha–C^\beta$ bonds of Ser[195] and His[57]. O^γ of Ser[195] can be "down" (torsional angle χ_1 about $C^\alpha–C^\beta$ of Ser[193] of $-80°$) or "up" (torsional angle χ_1 of $+90°$).[130,135,137-141] There exists, however, some controversy over the degree of conformational flexibility in the Ser[195] side chain.[130] Most other serine proteases appear to have the Ser[195] side chain in the down position ($\chi_1 \approx -80°$). Thus, for the active-site serine group, α-lytic protease has χ_1 $-56°$,[138] *Streptomyces griseus* serine protease (SGPA) has χ_1 $-77°$,[139] and native subtilisin has χ_1 $-100°$.[140] In the latter, however, the $C^\alpha–C^\beta$ bond for the active-site serine (Ser[221]) rotates by $+40°$ on going from native subtilisin to a tetrahedral intermediate boronic acid complex,[139] which involves movement of O^γ of Ser[221] by 1 Å. In one peptide product protease complex (Ac-Pro-Ala-Pro-Tyr-OH SGPA) Ser[195] appears to occupy two sites. A minor

occupancy site ($<20\%$) appears to have χ_1 for Ser[195] of $+35°$ while the major site has a normal χ_1 value of $-86°$.

The imidazole ring of His[57] can exist in two distinct positions as well. In trypsin–pancreatic trypsin inhibitor complex, the imidazole ring is found in the "in position" (torsional angle χ_1 $+62°$) about $C^\alpha–C^\beta$ of His[57] while in trypsin–benzamidine complex (T–B) and tosyl chrymotrypsin (T–C) the imidazole ring is in the "out position" (χ_1 of $+92°$ and $+97°$, respectively). In the free enzyme, O^γ of Ser[195] hydrogen bonds to $N^{\epsilon 2}$ of His[57] (part of the much debated "charge-relay" system[130] or "proton-relay" system[142]) in a conformation that places it too far from the carbonyl carbon C' of the substrate. Blow provides for simple rotation about $C^\alpha–C^\beta$ in a direction opposite to that depicted so as to bring C' and O^γ into bonding distances ($98 \rightarrow 99$, Figure 8) in a line roughly perpendicular to the plane of the trigonal carbon C' (as required by X-ray modeling studies and calculations[143-146]). Blow's rotation and attack would first form a tetrahedral intermediate closer in structure to intermediate **100** except that the H bond would still exist between O^γ Ser[195] and His[57] as shown in **99**. This conformation for **99** about $C^{\alpha195}–C^{\beta195}$, $C^{\beta195}–O^{\gamma195}$, and $O^{\gamma195}–C'$ in the HN–$C^\alpha–C^\beta–O^\gamma–C'–N'$ fragment would be g^-,g^+,g^+. Our suggested opposite rotation about $C^\alpha–C^{\beta195}$ also requires either a dip of C^β (requiring torsion about the Ser[195] side-chain bonds) or upward, to-the-right, movement of N' and C'. This approach would not necessitate displacement of His[57], which would otherwise get too close to O^γ (as mentioned by Blow). The resulting torsional angles in **99** about $C^\alpha–C^\beta$, $C^\beta–O^\gamma$, and $O^\gamma–C'$ are g^+,g^-,t. Without major displacements of any atoms, rotation about $C^\alpha–C^\beta$, $C^\beta–O^\gamma$, and $O^\gamma–C'$ gives the g^-,g^+,g^+ (**100**) conformation. The *compensating* opposite sense of rotation about $C^\alpha–C^\beta$ and $C^\beta–O^\gamma$ is similar to related pH-dependent backbone movements in α-CT.[142] Movement of His[57] from the in position to the out position allows the hydrogen bond from $N^{\epsilon 2}$ of His[57] to switch from the O^γ of Ser[195] to the leaving group N'. Thus, in the in-position the hydrogen bond between $N^{\epsilon 2}$ of His[57] and O^γ of Ser[195] is 2.7 Å and linear while the distance of $N^{\epsilon 2}$ to the nitrogen is too long (4.2 Å).[64] In the out-position the hydrogen bond is between $N^{\epsilon 2}$ and the leaving group N' (linear and 2.9 Å).[64] Cleavage of the scissile, C'–N' bond and formation of the acylenzyme **101** completes the first acylation steps. Addition of H_2O to **101** and reversal of the steps to **98** carry the reaction through to hydrolysis.

The only major difference between Blow's scheme and that shown in Figure 8 consists of a different conformation about HN–$C^\alpha–C^\beta–O^\gamma–C'–N'$H in the two tetrahedral intermediates **99** and **100**. The conformations in **99** about C'–N and $O^\gamma–C'$ are gauche and trans, respectively (g,t), which would be the optimum, stereoelectronically favored conformation for translation (either bond making or breaking) along the $O^\gamma–C'$ bond. Thus, initially the N'–H is trans to the carbonyl in the amide substrate and pointing toward $N^{\epsilon 2}$ of His[57] in **98** and as O^γ approaches to form **99**, the now pyrimidalized N' will have the N' lone pair (which is pointing toward solvent) app to the translating $O^\alpha–C$ bond. The stereoelectronic effect will thus lower the energy of this transition state.

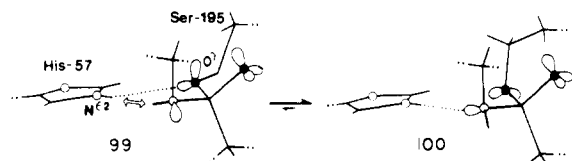As pointed out by Bizzozero and Dutler,[64] the leaving group N'–H is pointed toward the $N^{\epsilon 2}$–H bond, which

Figure 9. Redrawing of structures **99** and **100** of Figure 8 to clarify app lone pairs to $C'-O^\gamma$ scissile bond (a) and $C'-N'$ scissile bond (b). Reproduced with permission from ref 13. Copyright 1984 Rockefeller University Press.

would generate dipole–dipole repulsion between these groups (another perspective for structures **99** and **100** is shown in Figure 9). At the same time in **99** there are no lone pairs (or the incipient H-bonded lone pairs) app to the $C'-N'$ bond. This is required by the counterbalancing stereoelectronic effect. Our assumed conformation for intermediate **99** differs from Bizzozero and Dutler's[64] in not having a long pair on O^γ app to the $C'-N'$ bond. This particular conformation eliminates the app lone-pair interaction with the $C'-N'$ bond (and hence eliminates any counterbalancing stereoelectronic effect). However, it is not really necessary to assume that χ_1 must have a value of $+60°$ (g^+) in **99** to minimize this counterbalancing stereoelectronic effect in the $C'-O^\gamma$ bond-making transition state. A $40-60°$ rotation about the $C'-O^\gamma$ bond (with concomitant $40-60°$ counteracting rotation about Ser^{195} $C^\alpha-C^\beta$) will also considerably reduce the app lone-pair overlap with the $C'-N'$ bond. (Equation 2 shows that the overlap will follow a $\cos^2 \theta$ dependence of the dihedral angle θ between the interacting orbitals). As discussed above, χ_1 variation for Ser^{195} is just about this large in various modifications of the serine proteases. Especially notable, besides the large α-chymotrypsin χ_1 variation, is the pH dependence of the conformation of trypsin's Ser^{195}, with a value of $-95°$ at pH 5 and $-60°$ at pH 8.[131]

Experimental support for the stereoelectronically favored conformation about the $C'-N'$ bond (app lone pair to the translating $C-O^\gamma$ bond) is provided by Bizzozero and Zweifel's observation[63] of the lack of reactivity of peptide substrates, such as **102a** and **102b**, possessing an alkyl substituent on the leaving-group nitrogen.
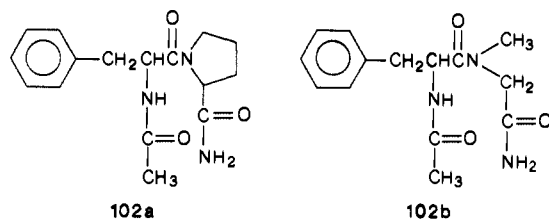
As discussed by Dugas and Penney,[147] both products were found to be unreactive but proved to be good competitive inhibitors of a specific substrate, N-Ac-L-Phe-OMe. This indicates that they form enzyme–substrate complexes of normal stability and that the reason for their unreactivity has to be sought in the nature of the enzyme–substrate interactions occurring during the subsequent bond-making and -breaking steps. In other words, their unreactivity can be understood by considering the stereoelectronic course of the transformation leading to the acylenzyme intermediate.

The attack of a trans peptide bond by the hydroxyl of Ser^{195} of α-chymotrypsin will give the steric situation depicted in Figures 8 and 9 and also in Scheme XI,

which has been proposed by Deslongchamps and discussed by Dugas and Penney.[147] The proposal in Figures 8 and 9, based on molecular orbital calculations,[13,62] agrees with the proposal in Scheme XI (with some modification about $HN-C^\alpha-C^\beta-O^\gamma-C'-N'H$ conformation in Scheme XI).

The important point to be considered here (Scheme XI) is again that the nonbonded pair of electrons on the nitrogen atom points toward the solvent (app to the Ser $O^\gamma-C'$ bond) and the $N-H'$ bond toward the inside of the enzyme active site. The distance between the leaving nitrogen and the imidazole ring in the tetrahedral intermediate is only 3.5 Å and is just sufficient to accommodate a hydrogen atom. When the N–H hydrogen is replaced by an alkyl group, as in the case of a proline residue, this substituent would come too close to the imidazole ring of His^{57}. Hence, a dipeptide containing an alkyl substituent on the leaving nitrogen is inactive toward α-chymotrypsin hydrolysis because the steric hindrance prevents formation of the tetrahedral intermediate in the required configuration: in Scheme XI the H' on the leaving nitrogen must be replaced by an alkyl group (R), configuration **99** then becomes impossible because the distance between the nitrogen and the imidazole ring is only 3.5 Å, and then when H' is replaced by R, the lone-pair orbital on the nitrogen can never be antiperiplanar to the nucleophile (Ser OH), preventing nucleophilic attack by Ser OH.

Inversion of pyrimidal nitrogen atoms carrying only hydrogen or carbon substituents is normally a very rapid process. The equilibrium between the two tetrahedral intermediates (**99**, **100**) of Figures 8 and 9 and Scheme XI is likely to be largely on the side of conformer **100** since conformer **99** is destabilized by the unfavorable dipole–dipole interaction between the NH group of His^{57} and the NH group of the leaving nitrogen. In conformer **100**, this unfavorable interaction is replaced by a favorable hydrogen-bond interaction between the NH group of His^{57} and the lone-pair orbital of the leaving nitrogen. It is interesting to note that due to this particular equilibrium position the tetrahedral intermediate is soon locked into a configuration **100** where reversion to the enzyme–substrate complex is no longer possible, since the bond between O^γ (Ser^{195}) and the carbonyl carbon of the substrate no longer has an antiperiplanar lone-pair orbital on the nitrogen. This N-inversion step implies that the leaving nitrogen acts as a switch controlling which of the two critical bonds of the tetrahedral intermediate, the C–O bond or the C–N bond, is broken. In the switch position corresponding to conformation **99** of the nitrogen, C–O bond breaking (forming) is allowed by the stereoelectronic effect, whereas C–N bond breaking is prevented by lack of nitrogen protonation by the imidazole. In the other switch position (**100**) of the nitrogen, C–O bond breaking is forbidden by the stereoelectronic effect but the possibility of nitrogen protonation allows the C–N bond to be broken. Since the tetrahedral intermediate is more stable in the **100** than in the **99** conformation, its breakdown in the forward direction is favored over that in the backward direction. Thus, the functional significance of such a switch lies in a protein-controlled suppression of the reverse reaction.

The second consequence of the complex function of His^{57} is that its imidazole ring must be able to swing

between a position allowing formation of a hydrogen bond between N (His[57]) and the leaving nitrogen. This imidazole mobility is consistent with X-ray diffraction data of the stable enzyme species showing that the two extreme positions of this movement, the in-position and the out-position, can readily be occupied.

Summary. These steric and stereoelectronic arguments thus can help explain why a proline residue involved in a peptide bond is resistant to α-chymotrypsin cleavage. Similar results have also been obtained for α-chymotrypsin-catalyzed hydrolysis of N-methylanilide substrates.[148]

Again, if the g,t conformation **99** is stereoelectronically best for lowering the energy of the transition state for O^γ bond formation, as discussed above, it must be the worst for C'–N' bond cleavage. The conversion of structure **99** to **100** assumes torsion about the Ser[195] bonds, histidine movement, and leaving-group nitrogen inversion and, in so doing, now places the $C^\beta O^\gamma$–C'–N'C fragment into the t,g conformation **100**. The down conformation for the Ser O^γ with χ_1 –80° and the out position for the imidazole group are now the same as that found in the X-ray structures for the T–B and T–C complexes.[131,132,135,137] Movement only of the now-protonated His[57] imidazole to the out position still would not permit it to protonate the leaving-group nitrogen since the NH is pointed toward the imidazole (see Figure 9 and Scheme XI). However, nitrogen inversion[63,64] allows the leaving-group nitrogen lone pair to point toward the imidazole instead of toward the solvent. Although the O^γ–C'–N'–C torsional angle is still gauche, nitrogen N' inversion changes the O^α–C'–N'–H torsional angles from gauche to trans. The conformation in **100** is thus described as t,g even though the trans designation refers to the O^γ–C'–N'–H dihedral angle. In the tetrahedral intermediate **100** the N'–H bond is now app to the O^γ–C' bond, whereas in **98** and **99** the lone pair was app to this bond. The stereochemistry of this N'–H bond is clearly defined by its hydrogen bonding to the carbonyl of Cys[191].[130,138] Recall in the transition state to **99** we identified the N' app lone pair to O^γ–C' as stereoelectronically controlling O^γ–C' bond translation. The trans N'–H to the C' carbonyl oxygen on the planar amide system must at some stage during either the nitrogen pyrimidalization process **98** → **99** → **100** stage move from a position pointing toward His[57] to the normal position away from His[57] and hydrogen bonding to Cys[191]. In the N' pyrimidal state **99** or **100** simple nitrogen inversion suffices, but in approaching the first transition state from **98**, this should not be possible and the NH should stay on the side facing His[57] and trans to C'=O. The unfavorable interaction of the N' app lone pair in **99** with the carbonyl oxygen of Cys[191] may in fact be yet another factor in stabilizing the first transition state. Once the intermediate **99** is formed, inversion to **100** is possible.

It must be stressed that the g,t → t,g conformational change of the tetrahedral intermediates (**99** → **100**) can be achieved with minimal distortion of the enzyme-bound substrate. The proposal that the serine side group must be capable of attaining various conformations to allow for full reactivity is not unrealistic considering the known variability of its orientation in various crystalline forms as shown by X-ray diffraction studies. Thus, the χ_1 (C^α–C^β) torsional angle can vary

SCHEME XII
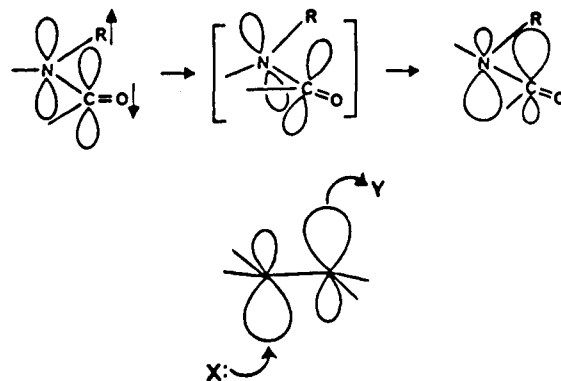
between +93° (pH 4.5, native α-CT)[130] and −83° (in the pH 8.0, native trypsin and T–C[135,137]). These differ substantially from the torsional angles in the trypsin inhibitor complexes and are consistent with those proposed in **99** and **100**. Thus, substantial variation *is* possible. Together with the mechanistically required nitrogen inversion and the observed flexibility in the imidazole group, it would appear as though the serine proteases are designed to provide the stereoelectronically optimal transition states for both the acyl addition *and* elimination steps.

C. Torsional-Strain Considerations. Carboxypeptidase A

Mock[5] emphasized the importance of torsional strain in enzymology, leading to a unique mechanistic hypothesis for proteolytic cleavage by carboxypeptidase A. According to his analysis, torsional deformation of the peptide linkage by anti distortion of cis substituents (i.e., forcing groups attached to one side of an amide partial π bond out of plane in opposite directions) leads to rehybridization of the constituent atoms (nitrogen and carbonyl carbon) toward tetrahedral geometry. In consequence the partial π bond is uniquely activated toward trans (antarafacial) addition with defined steric orientation of addends. Consider the case in which the cis substituents of a partial π bond are drawn away from opposite faces of the functional group (see Scheme XII). Such a distortion could easily be induced to a moderate extent by intramolecular forces involved in enzyme-substrate binding. The critical realization is that a pure torsional response (figure in brackets in Scheme XII), with retention of sp² hybridization and a diminution of $p\pi$–$p\pi$ overlap, is a naïveté. In actuality, a modest rehybridization of the unsaturated atoms will occur (sp² → sp^{2–3}). This has the primary effect of bringing the axes of the (predominantly) p atomic orbitals back generally into parallel; the resultant gain in π overlap compensates for expense of incorporation of some s character. Of particular relevance is the observation that it is orbital lobes on opposite faces of the partial π bond that are expanded in this mode of molecular distortion. It is the chemical consequences of this latter result that are significant.

His only assumption is a simple one: for a concerted addition to such a strained double bond as described above, attack will be upon the expanded atomic orbital lobes (i.e., maximum overlap considerations dictate the lowest energy reaction path). It follows that (a) trans
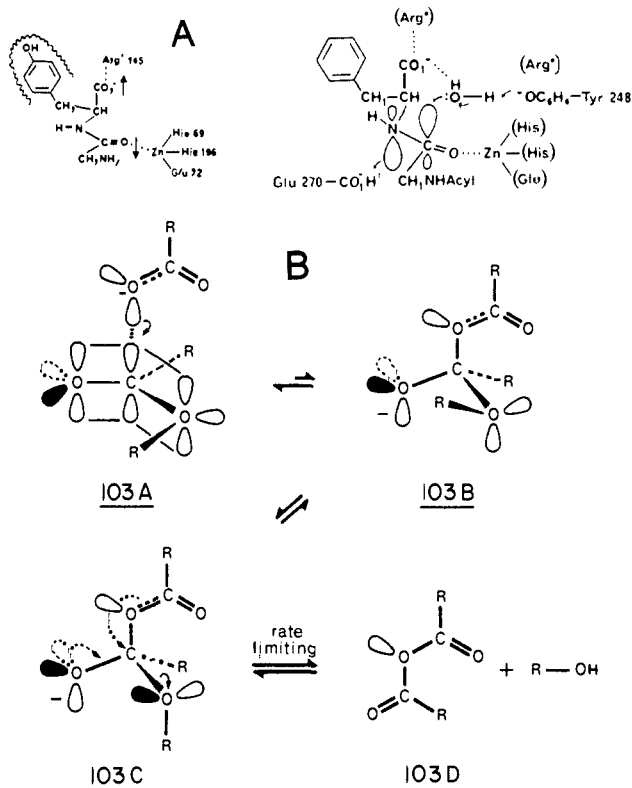
Figure 10. A. Proposed mechanism of action of carboxypeptidase A catalyzed hydrolysis of a peptide substrate, based upon the torsional strain hypothesis of Mock.[5] In contrast to other suggested mechanisms for this enzyme, this mechanism attempts to incorporate the required rehybridization of the amide linkages from stereoelectronic considerations. This suggests that Glu^{270} acts as a proton donor. Reprinted with permission from Mock.[5] Copyright Academic Press 1985. B. Proposed mechanism of action of carboxypeptidase A catalyzed hydrolysis of an ester substrate, based upon Makinen's stereoelectronic analysis. Reproduced with permission from ref 2. Copyright 1983 Pergamon.

(antarafacial) addition will occur exclusively in the situation described previously and (b) a clear distinction can be made with regard to which face the respective addends (X, Y) will approach in the case of a polar π bond such as an amide (i.e., stereoselectivity will be coupled with regiospecificity). It is noteworthy that Mock's torsional-stain consideration is equivalent to the stereoelectronic effect. The significance of the stereo and regiospecificity imposed by this torsional effect has led Mock to suggest an interesting mechanistic hypothesis for carboxypeptidase A (Figure 10A).[5]

Makinen also discussed the torsional distortion/stereoelectronic effect in the context of a more "traditional" mechanism of action for carboxypeptidase A[149,150] (Figure 10B). Based upon magnetic resonance studies of a spin-labeled substrate and computer graphics molecular modeling, Makinen and co-workers suggested that conformer **103A** is in the proper stereoelectronic conformation to break down to yield either the free substrates or the mixed-anhydride intermediate **103D**. Breakdown of conformer **103C** should, however, only give the mixed-anhydride enzyme complex. These authors suggest that torsional distortion of the substrate drives the conformational change **103B** → **103C**, which involves a simple single-bond rotation. Similar torsional activation following stereoelectronic principles can also be applied to carboxypeptidase A catalyzed hydrolysis of peptide substrates.
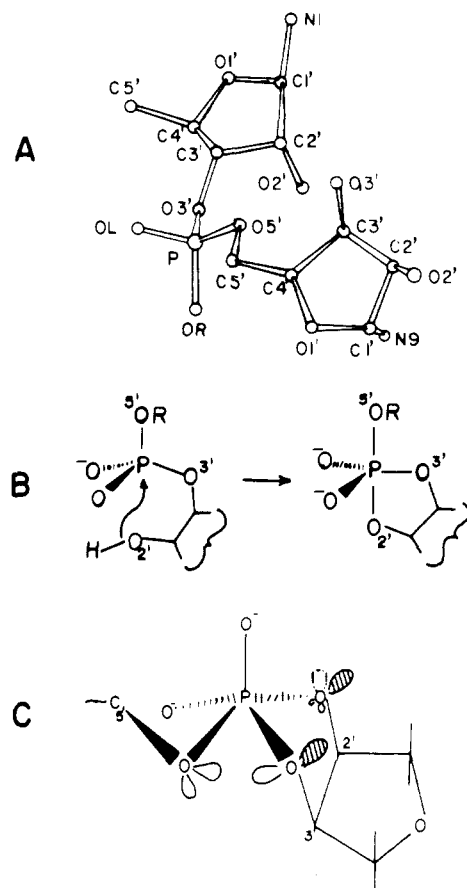
Figure 11. (A) Structure of the U^{33}-2'-OMeG^{34} dinucleotide portion of phenylalanyl tRNA. Only the diribose phosphate is shown. (B) "In-line" mechanism for attack of 2'-OH at phosphorus to form five-membered-ring pentacovalent intermediate in RNase-catalyzed hydrolysis of RNA. (C) Possible tetragonal-pyramid transition state for the transesterification step of RNase A. Lone pairs on O3' and O2' app to P-O5' are shaded. Only slight distortion ($\leq 15°$) of the bond angles is required to convert this structure into an in-line basal-in, basal-out trigonal-bypyramid transition state (apex P-O, O2', O5' in the basal plane with O3' and the other P-O apical). Reprinted with permission from ref 18. Copyright American Chemical Society 1977.

D. RNase A

It is likely significant that pancreatic RNase A preferentially cleaves yeast phenylalanyl transfer RNA (tRNA) at only two positions along the chain.[151] One point of attack is the internucleotide linkage 74-75 which, being at the end of the chain, is relatively flexible, and the other is the linkage between uridine-33 and $O^{2'}$-methylguanosine-34. , The X-ray structure[152-154] shows this internucleotide phosphate in a g,t conformation. Although other conformations for phosphate ester bonds with 3'-pyrimidine bases are found at the surface of the tRNA molecule, only this conformationally restricted diester is attacked by RNase A. (For example $C^{56}G^{57}, U^{68}U^{69}, U^{69}U^{70}, C^{70}G^{71}$ internucleotide phosphates in the double helical acceptor stem and $T\Psi C$ loop are potentially quite accessible to RNase A, yet none of these diesters in a g,g conformation are cleaved by the enzyme). Furthermore, as shown in Figure 11A, it is the 5' bond of the dinucleotide that is in the trans conformation and the 3' bond that is in the gauche conformation. Since only the 5' bond is ever cleaved by RNase A, the enzyme has fully taken advantage of the stereoelectronic consequences of the g,t conformation. Not only is P-O5' weakened and P-O3'

strengthened (thus preventing its breaking), but also the electron density on the 5'-oxygen is higher in this conformation than on the 3'-oxygen.[18] Protonation by one of the active-site histidines (presumably His[119]) would thus be facilitated. In addition, the g,t conformation is slightly higher in energy than the lowest energy g,g conformation, which should induce strain in the substrate and hence further accelerate the enzymatic reaction. Finally, the optimized ester RO–P–OR bond angle in the g,t conformation is 5–6° smaller than in the g,g conformation, and therefore distortion in the direction of the trigonal-bipyramid transition-state geometry (RO–P–OR bond angle, 104–90°) is achieved. Note that the bond angle is also closer to that of the 2',3'-cyclic nucleotides (98°),[155] where the reduced bond angle is likely an important factor in the 10^6 times faster hydrolysis of the strained five-membered cyclic phosphates.[98]

One additional point must be considered in this mechanism since the tRNA, U^{33}-2'-OMeG^{34} dinucleotide fragment is not in the correct conformation for an "in-line" or backside attack by the 2'-hydroxyl group as appears required in the RNase-catalyzed reaction[156] (Figure 11B). However, rotation of the uridine-33 ribose ring by ca. 180° about a rough axis through the C5'–O5' and C3'–O3' bonds does line the 2'-hydroxyl group backside to the departing 5'-ester bond. After this rotation of the ribose ring (presumably reflecting a conformational change of the enzyme complex) the dinucleotide conformation is comparable to the X-ray structure of a dinucleotide analogue bound to RNase A.[157] Note in this synperiplanar conformation about the P–O3' ester bond relative to the *attacking* 2'-oxygen, both of the lone pairs on the 3'-oxygen are oriented partially app to the attacking bond (Figure 11B). As discussed in section IVC3, this is the stereoelectronically favored conformation for making (or breaking) this 2'-ester bond. Of course, it is just the stereoelectronically wrong conformation for breaking the 5'-ester bond. If the rate-limiting step in the enzymatic reaction were formation of the 2'-ester bond, then this analysis would be consistent with the stereoelectronic effect. Alternatively, with a mechanism involving a pentacovalent square-pyramid transition state[18] it is possible to simultaneously observe the stereochemistry of reaction and orbital overlap requirements for both making the 2'-ester bond, breaking the 5'-ester, and eventually breaking the 2'-ester bond to complete the catalytic mechanism (Figure 11C).

A recent kinetic study of the hydrolysis of various dinucleoside monophosphate substrates by RNase A appears to support these stereoelectronic effects.[158,159] Yakovlev et al.[158,159] showed that dinucleoside phosphates in which either the *pro-R* or *pro-S* proton of the 5'-CH$_2$ group of the 5-nucleoside is replaced by a methyl group are still quite reasonable substrates of RNase A. While K_m values for the *pro-R* or *pro-S* methyl-substituted dinucleoside monophosphate differ by less than a factor of 2, k_{cat} is 60 times larger for Cp(*pro-R*-Me)U than Cp(*pro-S*-Me)U. Other RNases also cleave the *pro-S* methyl derivatives up to 250 times slower than the *pro-R* methyl dinucleoside phosphate derivatives. These authors suggest that the rate difference between the diastereomers can be attributed to a stereoelectronic effect. They argue that methyl substitution in the

pro-S position prevents the enzyme-bound phosphate from readily attaining the stereoelectronically demanded conformation (Figure 11). It is not clear, however, that factors other than the stereoelectronic effect cannot be responsible for these differences.

E. Staphylococcal Nuclease

Staphylococcal nuclease (Nase) is both a DNA and RNA hydrolyzing enzyme, which, like RNase A, specifically cleaves the 5'-oxygen ester bond.[160,161] However, unlike RNase A, a cyclic diester intermediate is not a prerequisite (and stereochemically complicating) feature of its mechanism of action. A rather dramatic demonstration of the specificity of Nase for cleaving only the 5'-bond is shown by the Nase-catalyzed hydrolysis of thymidine 3'-phosphate, 5'-*p*-nitrophenyl phosphate (**104**), which yields *only* p-nitrophenyl phosphate and 3'-thymidine monophosphate.[162]

104

105
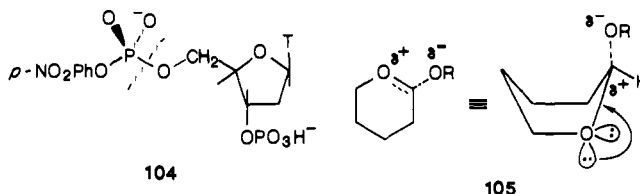
This contrasts dramatically with the nonenzymatic hydrolysis of this substrate, which because p-nitrophenoxide is a much better leaving group than the 5'-alkoxide yields thymidine 3',5'-diphosphate and p-nitrophenol.[162] While certainly other explanations are possible, one way in which the enzyme can achieve this specificity is to take advantage of the torsional activation *and* stabilization of the different ester bonds of a diester constrained to a g,t conformation.

It is significant, therefore, that based upon the Nase X-ray structural results of Cotton and co-workers[160,163,164] (Figure 12a) a phosphate diester substrate could bind to the enzyme in a g,t conformation, with the 5' bond in the trans conformation. As pointed out by Cotton, the rigidity and specificity of binding the 5'-phosphate is rather remarkable. Two arginine residues hydrogen bond to two of the phosphoryl oxygens of the 5'-phosphate. This suggested to us in our earlier analysis[18] that the remaining phosphoryl oxygen would normally be in the position of the 3'-ester oxygen of a natural diester substrate. Included in Figure 12a is an estimate of the allowed conformation for a 3'-ester group based upon an attempt to fit the rest of the DNA chain to the remaining open portion of the active site. This prediction appears to be supported by a later report at higher resolution (1.5 Å) for this complex.[164] The X-ray structure shows that, with a slight movement of atoms, the 5'-ester bond can be placed in the trans conformation while the 3'-ester bond could be in a gauche conformation. This conformation ensures that only the 5'-bond will be broken. Torsional catalysis capable of specifying which bond is to be broken may be especially important, since there does not appear to be a good acid group at the active site that can function as a general-acid catalyst to the 5'-alkoxide leaving group. Although Tyr[113] could serve this purpose, the enzyme is still quite active when the phenolic group is deprotonated, ruling out general-acid catalysis, at least by this group. Cotton et al.[164] suggested that the guanidinium ion of Arg[87] could be serving this purpose.
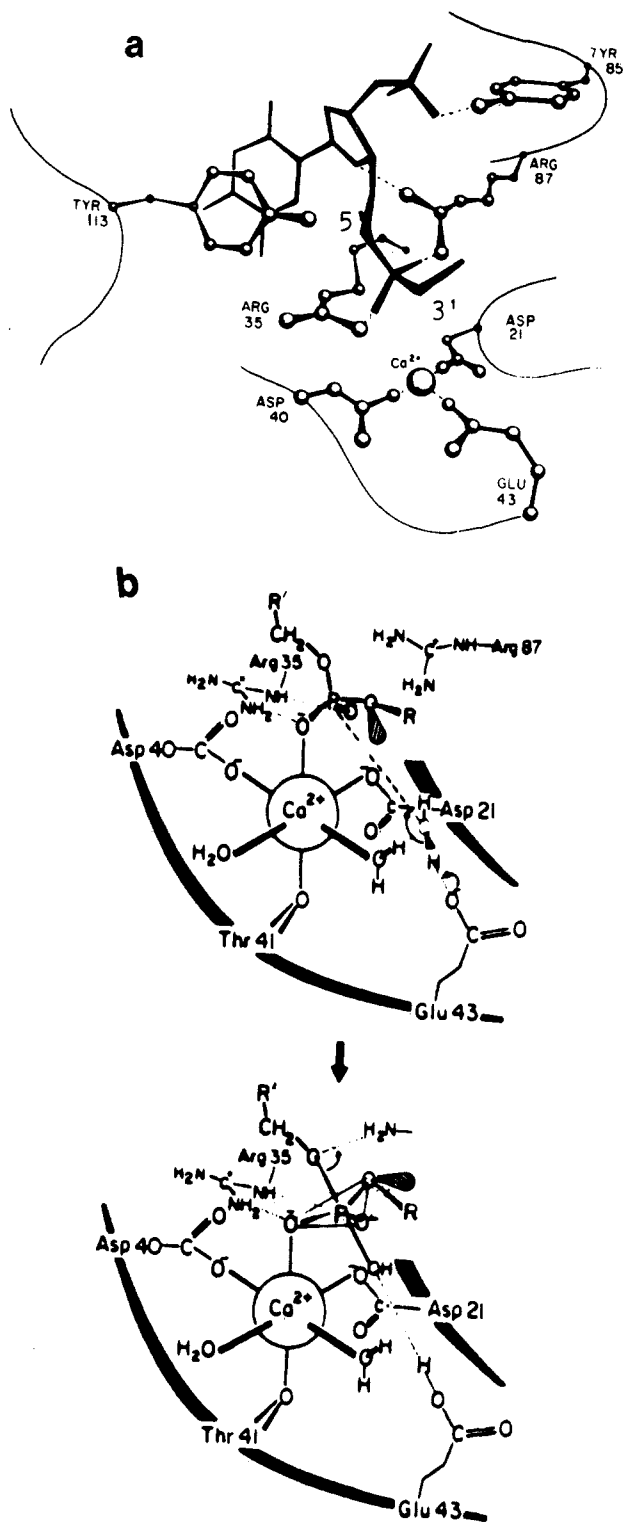
Figure 12. (a) Structure of the active site of staphylococcal nuclease and bound, 3',5'-pTp (adapted from ref 160). Reprinted with permission from ref 18. Copyright American Chemical Society 1977. A later, higher resolution X-ray structure[164] does not alter the basic stereoelectronic features of this figure. (b) Staphylococcal nuclease mechanism of Serpersu et al.[167] based upon the crystal structure of the 3',5'-pTp-enzyme complex.[164] The figure has been modified to show the app lone pair to the scissile 5'-ester bond.

Recent kinetic, NMR, and computer modeling studies on wild-type and site-specific mutants[165-167] of the enzyme appear to be generally supportive of this mechanism (Figure 12b). Note in Serpersu, Shortle, and Mildvan's mechanism of Figure 12b, a lone pair on the

3'-ester oxygen would be app to the 5'-ester leaving group, consistent with the stereoelectronic predictions. In the ground state, the phosphodiester is held by both Ca^{2+} and Arg^{35}, while Arg^{87} provides an additional interaction in the transition state.[167]

F. Stereoelectronic Effects in DNA Structure and Enzymatic Hydrolysis

It is now widely appreciated that duplex DNA can exist is a number of different conformations.[168] Significant conformational differences can exist globally along the entire double helix, as in the A, B, C, and Z forms of DNA.[168] In addition, local conformational heterogeneity in the deoxyribose phosphate backbone has been most recently noted in the form of sequence-specific variations[169-171] or as the result of drug[168] or protein binding[172-176] to local regions of the DNA.

It has been suggested that these localized, sequence-specific conformational variations are quite likely an important component of a DNA binding protein's recognition of specific sites on the DNA.[170,171,177] Thus, although the *lac* repressor protein does not recognize an alternating AT sequence as part of the *lac* operator sequence, the repressor protein binds to poly d(AT) 1000 times more tightly than to random DNA.[168] The repressor protein is quite likely recognizing the alternating deoxyribose phosphate backbone geometry of the two strands,[178] rather than the chemical identity of the AT base pairs. Endonucleases may also be able to induce unusual DNA conformations involving sharp bends[174-176] or kinks[173] in the duplex, and as described in the following, these structural variations may directly relate to an enzymatic stereoelectronic effect.[18,177]

1. Stereoelectronic Effect on [31]P Chemical Shifts as a Probe of DNA Structure

We noted that ^{31}P chemical shifts can potentially provide a probe of the conformation of the phosphate ester backbone in nucleic acids and nucleic acid complexes.[177,179-182] Molecular orbital calculations in our laboratory provided initial suggestions that ^{31}P chemical shifts were influenced by a stereoelectronic effect. This stereoelectronic effect on these ^{31}P chemical shifts is likely attributable to changes in the orbital populations (in turn affecting the charge and orbital unbalancing[182]) on phosphorus as a function of the conformation about the P–O ester bonds.[183] This appears to reflect a true stereoelectronic orbital effect, in which electron donation from the lone pairs on oxygen increases the electron density on phosphorus. Thus, the electron density on phosphorus is higher in the g,g phosphate diester (Figure 1) than in the g,t conformation. Later, a more theoretically justified, average excitation approximation approach confirmed the original calculation of a stereoelectronic effect on ^{31}P chemical shifts, with the prediction that the ^{31}P resonance of a phosphate diester in a g,g conformation should be several ppm upfield of the ^{31}P signal of an ester in a g,t or t,t conformation (Figure).[182] Pullman and co-workers[184] confirmed our earlier calculations of the isotropic ^{31}P chemical shifts with much more reliable gauge invariant ^{31}P chemical shielding tensor and isotropic chemical shift calculations.

Experimentally, the stereoelectronic effect on ^{31}P shifts can be confirmed by using six-membered-ring

model systems in which the torsional angles are rigidly defined by some molecular constraint, such as the two diastereomeric phosphate triesters 11a/b (as described in section IIB and shown in Table I).[37,43] Generally those diastereomeric phosphates with an axial ester group have ^{31}P chemical shifts as much as 6 ppm upfield from these isomeric phosphates with an equatorial ester group.[37,43] In 11b the equatorial ester group is locked into a trans conformation relative to the endocyclic P–O ester bond. Again, trans esters are downfield of gauche esters such as 11a.

These initial theoretical and simple model results suggested that we might be able to use this stereoelectronic effect on ^{31}P chemical shifts as a probe of nucleic acid conformations. Thus, as described above, if ^{31}P chemical shifts are sensitive to phosphate ester conformations, they potentially provide information on two of the most important torsional angles that define the nucleic acid deoxyribose phosphate backbone. One of these, the P–O3' torsional angle, is also the most variable one in the B-form double helix and the other P–O5' torsional angle is one of the most variable in the A-form of the duplex.[168] Indeed, following the original suggestion of Sundaralingam[185] and on the basis of recent X-ray crystallographic studies of oligonucleotides, Saenger[168] noted that the P–O bonds may be considered the "major pivots affecting polynucleotide structure".

Our earlier ^{31}P NMR studies on poly- and oligonucleic acids[44,179-183] supported our suggestion that the base-stacked, helical structure with a gauche,gauche phosphate ester torsional conformation should be upfield from the random-coil conformation, which contains a mixture of phosphate esters in other nongauche conformations as well.

2. Variation of [31]P Chemical Shifts in Oligonucleotides

More recently we[177,186-189] and others[190-192] used a [17]O/^{18}O-labeling scheme to identify the individual ^{31}P resonances of oligonucleotides. These labeling studies allowed us to gain insight into the various factors responsible for ^{31}P chemical shift variations in oligonucleotides.[186-192] As discussed above, one of the major contributing factors that determines ^{31}P chemical shifts is the main-chain torsional angles of the individual phosphodiester groups along the oligonucleotide double helix. Phosphates located toward the middle of a B-DNA double helix assume the lower energy, stereoelectronically favored g−,g− conformation (the notation for the P–O ester torsion angles follows the convention of: Seeman, N. C.; Rosenberg, J. M.; Suddath, F. L.; Park Kim, J. J.; Rich, A. *J. Mol. Biol.* **1976**, *104*, 142–143) with ζ (P–O3' angle) given first followed by α (P–O5' angle). However, phosphodiester linkages located toward the two ends of the double helix tend to adopt a mixture of g−,g− and g−,t conformations, where increased flexibility of the helix is more likely to occur. Because the g−,g− conformation is responsible for a more upfield ^{31}P chemical shift, while a g−,t conformation is associated with a lower field chemical shift, internal phosphates in oligonucleotides would be expected to be upfield of those nearer the ends. Although several exceptions have been observed, this positional relationship appears to be generally valid for oligonucleotides where ^{31}P chemical shift assignments have been determined.[186-192] Thus, position of the phosphorus (ends
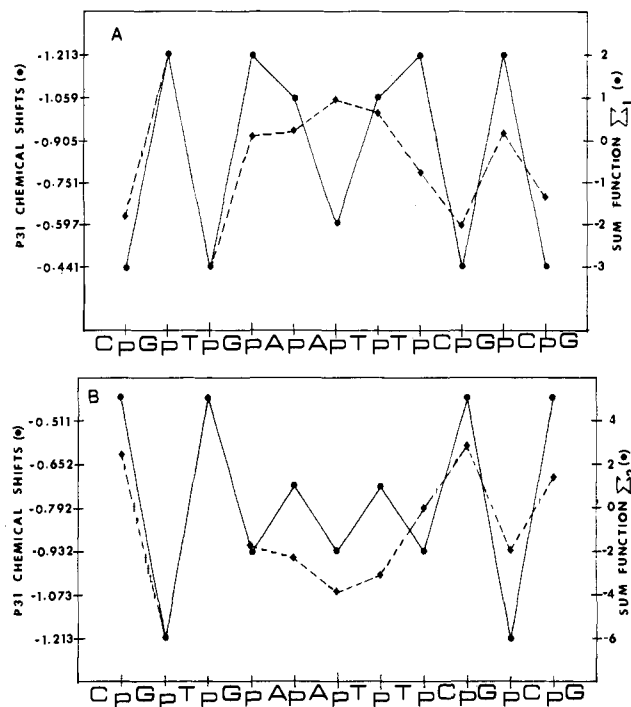

Figure 13. Correlation of Dickerson/Calladine rule sum functions for local helical twist (A) or roll angle (B) and ^{31}P chemical shifts for GT-mismatch 12-mer duplex (dCGTGAATTCGCG)$_2$.

vs. middle) within the oligonucleotide is one important factor responsible for variations in ^{31}P chemical shifts.

Ott and Eckstein[191,192] recently noted that the occurrence of a 5'-pyrimidine–purine-3' base sequence (5'-PyPu-3') within the oligonucleotide has a more downfield than expected ^{31}P chemical shift if based solely on the phosphate positional relationship. They suggested an explanation for these anomolous chemical shifts based upon sequence-specific structural variations of the double helix as proposed by Calladine.[169] As described in more detail below, local helical distortions arise along the DNA chain due to purine–purine steric clash on opposite strands of the double helix.[169] As a result, 5'-PyPu-3' sequences within the oligonucleotide represent positions where the largest helical distortions occur. Ott and Eckstein proposed, on the basis of the ^{31}P assignments of two dodecamers and an octamer, that a correlation exists between the helical roll angle parameter[169,170] and ^{31}P chemical shifts.[191,192] They noted a considerably poorer correlation between ^{31}P chemical shifts of the oligonucleotides and other sequence-specific variations in duplex geometry (such as the helix twist).

On the basis of ^{31}P assignments of oligonucleotides in our laboratory, we found that there does appear to be a reasonable correlation between ^{31}P shifts and the helical twist (as calculated from the helical twist sum function.)[177,188,189] (Figure 13). In fact, if we plot all of the assigned ^{31}P shifts of the six oligonucleotides from our laboratory and others,[191,192] a reasonable correlation appears to exist between ^{31}P chemical shifts and helical twist sum function (Figure 14).

The possible basis for the correlation between Calladine-rule parameters and ^{31}P chemical shifts can be understood from the following geometrical analysis. In order to increase the stacking overlap along each strand of a double helix, the bases along each strand are propeller twisted by 10–20° relative to the bases on the
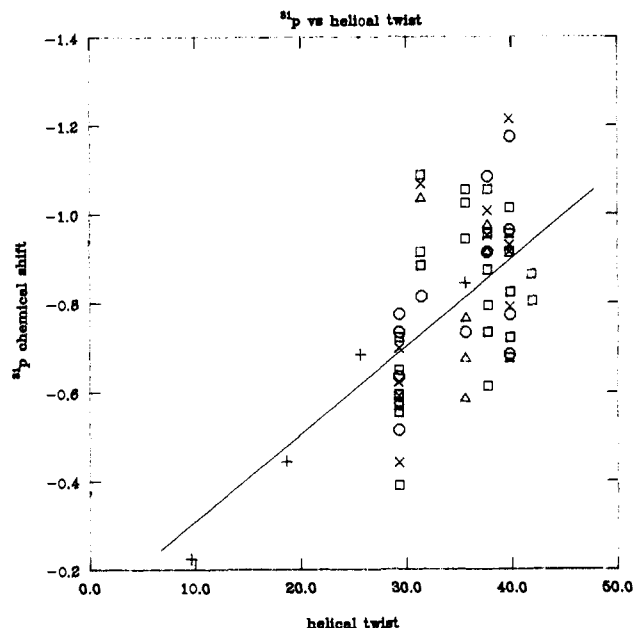
Figure 14. Plot of ^{31}P chemical shifts of assigned phosphates in duplex oligonucleotides dCGCGAATTCGCG[191,192] (□), dCGTGAATTCGCG[186] (×), dTGTGAGCGCTCACA[187] (○), dGGCCATATGGCC[191,192] (□), d(GGAATTCC)[191,192] (△), d-(CATGGATm⁵CCATG)[216] (□), as well as several drug–polynucleic acid complexes[217] (+) vs. calculated helix twist (t_g). t_g is derived from helix twist sum function ($\sum_1$) and $t_g = 35.6 + 2.1\sum_1$.[169-171] Two points at the site of m⁵G base pairs and base-pair mismatch in several of the oligonucleotides as well as the two end phosphates in the 8-mer duplex have been removed from the plot. The straight line is the best least-squares fit of the data.

opposite strand. Because the purines extend beyond the helix axis, in a 5′-purine–pyrimidine-3′ (5′-PuPy-3′) sequence of a 5′-PyPu-3′ sequence the purines on opposite strands that are separated by one base step sterically clash. The purine N2/N3 steric clash in the minor groove of a 5′-PyPu-3′ sequence is twice as severe as the steric clash of the purines in the major groove of a 5′-PuPy-3′ sequence, and hence a 5′-PyPu-3′ sequence produces the largest local geometry changes.[169-171]

Using a simple elastic beam mechanical model, Calladine[169] proposed four different conformational variations that will relieve this steric hindrance: (1) flattening the propeller twist; (2) opening the roll angle; (3) displacing the base pairs; (4) decreasing the local helix twist. These sequence-specific conformational variations will require changes in the deoxyribose phosphate backbone angles α–ζ:

$$P^\alpha\text{-}O5'^\beta\text{-}C5'^\gamma\text{-}C4^\delta\text{-}C3'^\epsilon\text{-}O3'^\zeta\text{-}P$$
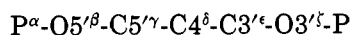
As the helix winds or unwinds, the distance between the adjacent C4′ atoms of deoxyribose rings along an individual strand ($D_{4'4'}$) must change to reflect the stretching and contracting of the deoxyribose phosphate backbone between two stacked base pairs.

Thus, decreasing the twist angle, t_g, from 36 to 25° reduces the steric clashing in the minor groove in a 5′-PyPu-3′ sequence by pulling the N2 and N3 atoms of the purines further apart. As the helix unwinds, the $D_{4'4'}$ separation decreases from ~5.8 to 4.7 Å (J. Metz, D. Gorenstein, unpublished). To a significant extent, these changes in the overall length of the deoxyribose phosphate backbone "tether" are reflected in changes in the P–O ester (as well as other) torsional angles.
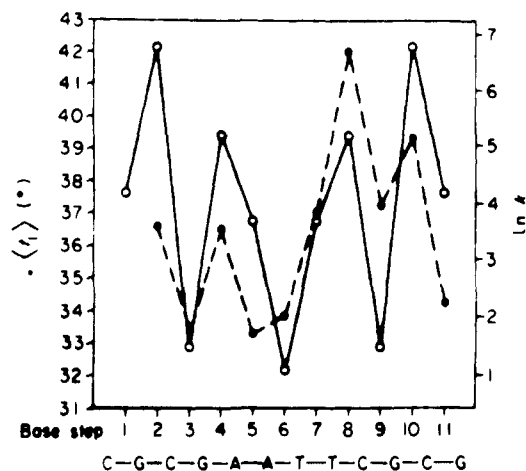

Figure 15. Correlation between local helical twist (t_g, ○) at a particular base step and the relative rate constant for cutting at that point by DNase I (ln k, ●). Rate data reprinted with permission from Lomonossoff.[194] Copyright Academic Press 1981. Figure reprinted with permission from ref 171. Copyright Academic Press 1983.

The sequence-specific variations in the P–O ester torsional angles may provide the linkage between the Calladine-rule-type sequence-dependent structural variations in the duplex and ^{31}P chemical shifts.

3. DNAse I: Significance of the Local Variation in Phosphate Ester Geometry

Of potential significance, Klug and co-workers[194] showed that the sites of DNAse I catalyzed hydrolysis of the palindromic 12 mer, d(CGCGAATTCGCG), correlates with the Calladine rules for sequence-specific local variation in duplex geometry (Figure 15). Drew and Travers[195] suggested that these sequence-specific variations in the DNA structure could be responsible for the specificity of DNAse I, DNAse II, and copper–phenanthroline-catalyzed hydrolysis of DNA. Although quite speculative, it may very well be possible that this dependence of the enzymatic (and nonenzymatic, copper–phenanthroline) catalyzed hydrolysis of the DNA to local helical structure[194,195] is a reflection of a stereoelectronic effect on phosphate ester hydrolysis. Thus, DNAse I has a very marked preference for hydrolyzing poly[d(AT)] on the 5′ side of T residues.[178,196] Based upon the crystal structure[197] of (d-AT)₂ and the DNAse I catalyzed hydrolysis of poly d(AT), Klug and co-workers[196] suggested that poly[d(AT)] exists in an "alternating-B" conformation. Significantly the ^{31}P spectrum of poly[d(AT)] gives two signals separated by as much as 0.8 ppm depending upon salt conditions.[198] By thiophosphoryl labeling, Eckstein and Jovin[193] were able to establish that the downfield shifted ^{31}P signal arises from the TpA phosphates, which based upon an X-ray crystal model are in a –60°, –125° phosphate ester conformation (later confirmed by a 2-dimensional NMR study[216] of poly[d(AT)]). The ^{31}P signal of the ApT phosphates is quite similar to that of a normal B-DNA phosphates and indeed is in a g⁻,g⁻ conformation. This downfield shift of the TpA phosphate is in agreement with the stereoelectronic effect on ^{31}P chemical shifts and consistent with the g⁻,ac conformation proposed by Klug and co-workers.[196]

Finally, the lack of enzymatic reactivity for the TpA phosphate could possibly be attributable to a kinetic

$$d(ApT)n \xrightarrow{\text{DNase I}} d(p-TpA)$$
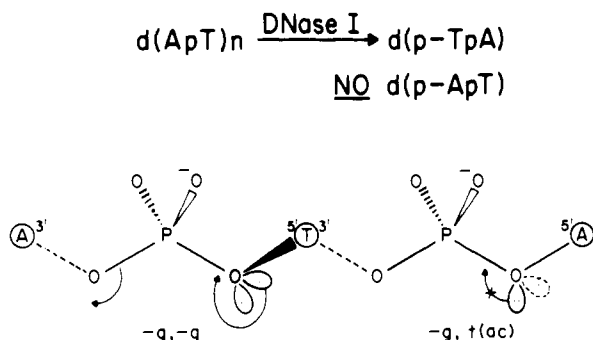$$\underline{NO} \quad d(p-ApT)$$

Figure 16. Schematic representation of phosphate ester conformation in poly[d(AT)] emphasizing the possible stereoelectronic control in providing regiospecificity to P–O ester cleavage in DNAse I catalyzed hydrolysis.
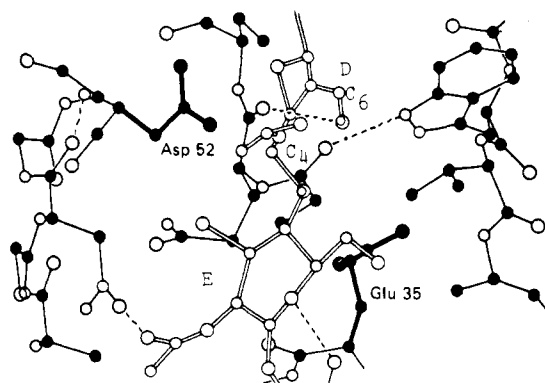

Figure 17. Structure of part of the active site of lysozyme, including rings D and E of a hexasaccharide substrate. Ring D is shown in the hypothetical sofalike conformation (adapted from ref 199). Figure reprinted with permission from ref 18. Copyright American Chemical Society 1977.

stereoelectronic effect. As shown in Figure 16, in a g,t conformation for the TpA phosphates, and to a lesser extent in a –60°, –120° conformation, neither of the lone pairs on the 5'-oxygen on the A residues would be app to the 3'-O–P ester bond which is cleaved by DNAse I. In contrast in the g⁻,g⁻ conformation for the ApT phosphate, one of the lone pairs on the 5'-oxygen of the T residues is app to the bond cleaved by the enzyme. Unfortunately, this "explanation" is not entirely consistent with the current "model" for the poly[d(AT)] duplex which places the 5'-ester bond in the g⁻ conformation and the 3'-ester bond in the ac conformation (the opposite of the stereoelectronic requirement for specific deactivation of the TpA 3'-ester bond). Whether, of course, these ³¹P and enzymatic correlations truely reflect stereoelectronic effects remains to be firmly established.

G. Lysozyme

Lysozyme cleaves the anomeric bond of an N-acetylglucosamine residue that binds to the D subsite of the enzyme (a total of six subsites are thought to comprise the total active site). On the basis of initial X-ray studies, Philips and co-workers originally suggested that distortion of the reacting sugar residue occurs upon binding[199] (Figure 17). In the commonly accepted "textbook" mechanism for lysozyme, the enzyme is suggested to force the sugar ring in subsite D into a half-chair or, in later interpretations, into a sofa or twist-boat conformation. Cleavage of the "strained"

SCHEME XIII
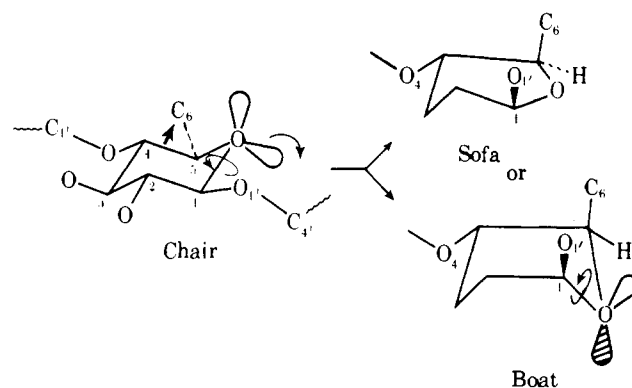
aglycon bond with general-acid catalysis by Glu[35] yields an oxycarbonium ion in the ring that is stabilized by the adjacent negative charge of Asp[52]. Much has been made of this strain or distortion catalysis in the enzymatic mechanism, although Warshel and Levitt[200] claimed that their calculations suggested that the distortion factor is of minimal importance[78,201] (Scheme XIII).

Binding studies[202] and X-ray studies on a tetrasaccharide lactone "transition-state" analogue originally provided support for the distortion mechanism, however. These models suggested that the C6 OH group of the sugar ring in subsite D must move out of its equatorial position to reduce severe steric interaction with the enzyme. Phillips argued that this forces the sugar ring into the sofa or boat conformation, with the C6 OH group moving into an axial position. In the chair conformation with a $\beta(1\rightarrow4)$ linkage the torsional conformation about the C1–O5 bond is trans, and hence according to our original predictions based upon stereoelectronic arguments, the wrong bond is disposed to cleavage.[18] (It is the aglycon C1–O4' bond that must actually be broken by the enzyme.) However, by distorting the ring into a boat conformation, the C1–O4' aglycon bond moves into an axial position along with the C6 OH group (the C6 OH group serves as the "arm" for this distortion). By pushing C1–O4' axial, the conformation about the C1–O5 bond moves from trans to gauche. In addition, inspection of the X-ray model of Phillips as reproduced in Figure 17 shows that the C1–O4' bond is in a trans conformation. Thus, the activated conformation for the anomeric carbon of a lysozyme-bound sugar is g,t, with the bond being broken being the weakened trans bond. These conclusions are approximately equally correct even if the sugar takes on a "sofa" conformation. Since these distorted conformations are ≥6 kcal/mol[199] higher in energy than the unstrained, normal chair conformation, significant catalysis is provided if this strain energy is utilized to move the enzyme–sugar complex structure along the reaction coordinate. Only in the boat or a distorted sofa conformation can an app lone pair on the ring oxygen be used to weaken the C1–O4' bond. In this way the increased overlap between the developing carbonium ion and the app lone pair on ring O5 stabilizes the oxycarbonium ion structure.

It should be noted that more recent binding studies[203-205] and molecular mechanics calculations[200] have suggested that no distortion of the D ring occurs or is even necessary for enzymatic catalysis. However, the
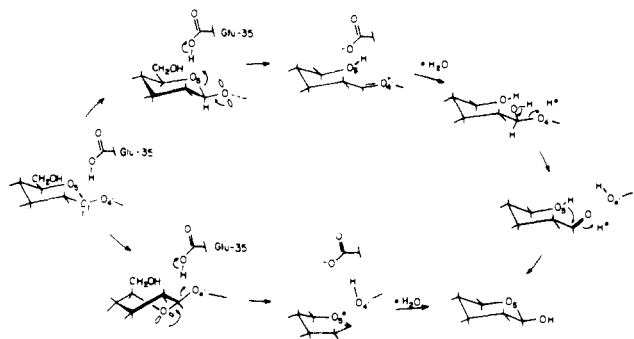
Figure 18. Generally accepted mechanism (Scheme II, bottom path) for lysozyme catalysis showing twist-boat conformation for ring D and app lone pair to the O4' leaving group. Alternative mechanism (Scheme I, top path) that attempts to reconcile stereoelectronic control mechanism and molecular dynamics simulations. Cleavage of the O5' acetal bond is facilitated by an app lone pair on the O4' ring oxygen. Reprinted with permission from ref 206. Copyright American Chemical Society 1986.

Figure 19. Plot of the stereochemical preference of dehydrogenases (*pro-R* or *pro-S*) vs. the negative logarithm of the equilibrium constant for the reactions they catalyze. K_{eq} = [H$^+$][NADH][ketone]/[NAD$^+$][alcohol]. Key to the figure is found in ref 209. Reprinted with permission from ref 209. Copyright Berkhaeuser 1983.

distortion mechanism does not require that the enzyme distort the *ground-state* enzyme-substrate complex into a twist-boat conformation. Again, as shown for the nonenzymatic reaction of flexible substrates, what is relevant is the extent of stereoelectronic control in the transition state (Figure 4). It may well be possible that the initial, lower energy, chair conformation enzyme-substrate complex isomerizes to a higher energy distorted twist-boat conformation.

Note that without proper app orbital orientation, the carbonium ion like transition state would *not* be stabilized by the adjacent oxygen atom. In fact, as discussed in section IVA the electron-withdrawing oxygen atom would destabilize a carbonium ion if proper orbital overlap were prevented. This would be the case if lysozyme catalysis occurred in the original, undistorted chair conformation.

A very intriguing, novel mechanistic suggestion by Post and Karplus[206] attempts to reconcile the apparently conflicting stereoelectronic arguments and the molecular dynamics simulations on a lysozyme-substrate complex and experimental data. In line with other energy minimization results,[200,207] the molecular dynamics calculations[206,208] argue against the substrate distortion mechanism (Figure 17; bottom path, Figure 18). In an alternative mechanism (top path, Figure 18), Post and Karplus propose that the endocyclic C1–O5 bond first cleaves with stereoelectronic assistance from an app lone pair on the O4' oxygen. In this way the stereoelectronic effect provides an entropic (section VA) advantage rather than the distortional enthalpic strain energy assumed by the earlier mechanisms.

Finally, these stereoelectronic considerations would lead us to predict that the mechanism of action of α-glucosidases in which the C1–O5 bond already exists in the proper gauche conformation probably does *not* involve severe distortion of the chair conformation. However, Hosie and Sinnott[201] claim that yeast α-glycosidase distort the ring into a conformation in which the lone electron pair is no longer app to the scissile bond.

H. Stereoelectronic Effects in Dehydrogenases

Benner[209–211] made the interesting suggestion that the stereoselectivity of dehydrogenases dependent upon the nicotinamide cofactors can be analyzed in terms of a
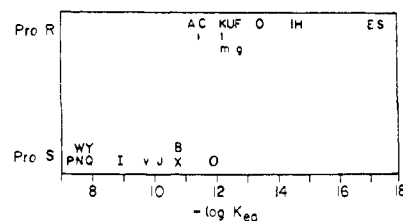
stereoelectronic effect. Westheimer, Vennesland, and co-workers made the significant observation 35 years ago that the dehydrogenases stereoselectively transfer only one of the hydrogens at the 4-position of the reduced form of the nicotinamide coenzyme.[212] Over the years, it appeared that this stereoselectivity among the different dehydrogenases was random, with some transferring the *pro-R* hydrogen and others the *pro-S* hydrogen. Benner has proposed that the transfer stereoselectivity is not random, but rather that for enzymatic redox reactions involving reduction of carbonyl compounds to alcohols, the *pro-R* hydrogen of NADH is used to reduce the thermodynamically unstable carbonyls while the *pro-S* hydrogen is used for the more stable carbonyls. Some of the data are reproduced in Figure 19. The mechanistic basis for this hypothesis rests on several assumptions: (1) The *pro-R* hydrogen is transferred from the nicotinamide ring bound in an anti conformation whereas the *pro-S* hydrogen is transferred from the ring bound in a syn conformation. (2) The NADH is a weaker reducing agent when it is in an anti conformation than when it is in a syn conformation. (3) As discussed in section VA, enzymes (presumably including the dehydrogenases) that are "evolutionarily perfected"[121] have evolved so as to match the free energies of the bound intermediates.

Benner bases his first assumption on stereoelectronic principles. Thus as shown in Figure 20a, the anomeric effect (or really the exo-anomeric effect) will favor a conformation in which the lone pair on nitrogen will be app to the polar sugar C–O bond, and this should distort the reduced nicotinamide ring into a boat conformation (although this point has been debated[213]). When the boat nicotinamide ring is in the anti conformation, the *pro-R* hydrogen is in a pseudoaxial position, whereas the *pro-S* hydrogen is pseudoaxial when the ring is in the syn conformation. The stereoelectronic effect also allows prediction that the pseudoaxial hydrogen will be most easily transferred, since the orbital containing the transferring hydrogen will be better able to overlap with the adjacent π orbitals.[214] (Figure 20b). These stereoelectronic arguments, plus assumptions 2 and 3, have led Benner to conclude that the dehydrogenase utilize the *pro-R* hydrogen of anti NADH (representing a weaker reducing agent) to reduce the more reactive carbonyls. The *pro-S* NADH is a stronger reducing agent and reduces the less reactive carbonyls. This allows a match between the energies of the bound intermediates.

Oppenheimer[213] and You[215] raised concern about the validity of this correlation between the stereospecificity of the dehydrogenases and the equilibrium constant for
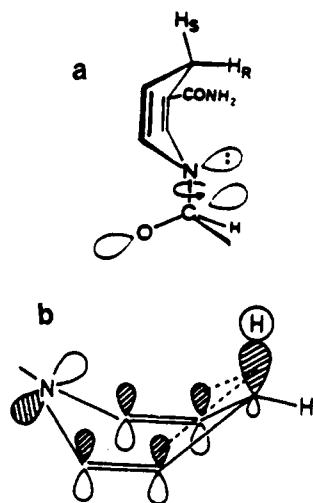
Figure 20. (a) Hypothesized[209] stereoelectronic origin of boat conformation for nicotinamide ring in NADH. In this exo-anomeric effect, the lone pair on nitrogen will best overlap with the antibonding σ^* orbital of the sugar C–O bond if the reduced nicotinamide ring is in the boat conformation. This places the *pro-R* hydrogen at the 4-position in a pseudoaxial position when the ring is in the anti conformation and the *pro-S* hydrogen in the pseudoaxial position when the ring is in the syn conformation. Reprinted with permission from ref 210. copyright American Chemical Society 1983. (b) Stereoelectronic origin of the putative[209] enhanced reactivity for the pseudoaxial hydrogen in the boat conformation of the reduced nicotinamide ring in Figure 20a. Instead of an app lone pair on a polar heteroatom, the π-type HOMO of the π-system can overlap with the antibonding σ^* LUMO of the axial scissile C–H bond in the boat conformation. Shading of the orbitals indicates the relative sign of the orbital lobes. Reprinted with permission from ref 214. Copyright American Chemical Society 1984.

the reaction. In particular, there appear to be several enzymes that do not conform to the predictions. Benner and co-workers[211] rebutted these challenges, arguing that the substrates chosen in those reactions that appear to be in violation of the theory are not the "natural" substrates. In fact of 130 dehydrogenase enzymes, 120 apparently fit Benner's correlation and five do not. The theory would therefore at the very minimum have remarkable predictive utility. Experimental support for the stereoelectronic arguments may also be found.[211,214]

VI. Conclusion

In spite of the large body of theoretical and experimental data supporting the stereoelectronic effect in the reactions of carbon and phosphorus compounds, significant controversy continues to exist. Much of the controversy centers on the variation in the magnitude of the stereoelectronic acceleration in rate-determining and product-determining steps. Estimates of ≥ 1 to 10 kcal/mol or more can be found in the literature. It is now becoming clear, however, that problems of conformational flexibility in various systems can readily mask any attempt to assess the importance of the stereoelectronic effect. This was shown in the *trans*-decalin type ring system phosphate triesters,[36,37] where low-energy twist-boat conformations confound any effort to quantitate the stereoelectronic effect. Kirby and co-workers[69-72] came to similar conclusions in the hydrolysis of various cyclic acetals. However, in more rigid systems such as five-membered ring systems **69** and **80/81** and highly constrained bicyclic ring systems such

as **56/58** and **63**, rate accelerations in rate- and product-determining steps of 10^2–10^3 or even greater can be found. Unfortunately in any of these systems, one can always envision some other possible explanation for the rate accelerations. Similarly, it is possible to argue that most compounds that can orient one or more lone electron pairs app to a reactive bond react via a stereoelectronically favorable conformation. So long as these stereoelectronically kinetically favorable non-ground-state conformations or intermediates are lower energy than the transition state(s) for a reaction, then the reaction will follow a stereoelectronically assisted pathway. An entropic penalty must be paid, but so long as the enthalpic advantage of lowering the transition-state energy through a stereoelectronic effect is there, one cannot rule out the importance of a stereoelectronic effect in acyclic or conformational flexible cyclic systems.

In the end, many more tests of the stereoelectronic effect in biological systems are clearly required. As we continue to build up a body of experimental evidence supportive of this theory, we will hopefully be in a position to predict contributions of the stereoelectronic effect to the structure and reactivity of biomolecules.

VII. Acknowledgment

VIII. Literature Cited

(1) Deslongchamps, P.; Taillerfer, R. J. *Can. J. Chem.* **1975**, *53*, 3029.
(2) Deslongchamps, P. *Stereoelectronic Effects in Organic Chemistry*; Pergamon: Oxford, 1983.
(3) Kirby, A. J. *The Anomeric Effect and Related Stereoelectronic Effects at Oxygen*; Springer-Verlag: Berlin, 1983; pp 1–149.
(4) Storm, D. R.; Koshland, D. E., Jr. *J. Am. Chem. Soc.* **1972**, *94*, 5815.
(5) Mock, W. L. *Bioorg. Chem.* **1985**, *4*, 270.
(6) Lehn, J. M.; Wipff, G. *J. Chem. Soc., Chem. Commun.* **1975**, 800.
(7) Lehn, J. M.; Wipff, G. *J. Am. Chem. Soc.* **1974**, *96*, 4048–4050.
(8) Lehn, J. M.; Wipff, G. *J. Am. Chem. Soc.* **1976**, *98*, 7498.
(9) Lehn, J. M.; Wipff, G. *Helv. Chim. Acta* **1978**, *61*, 1274.
(10) Lehn, J. M.; Wipff, G. *J. Am. Chem. Soc.* **1980**, *102*, 1347.
(11) Radom, L.; Hehre, W.; Pople, J. A. *J. Am. Chem. Soc.* **1972**, *94*, 2371.
(12) Jeffrey, G. A.; Pople, J. A.; Radom, C. C. *Carbohydr. Res.* **1972**, *25*, 117.
(13) Gorenstein, D. G.; Taira, K. *Biophys. J.* **1984**, *46*, 749–762.
(14) Gorenstein, D. G.; Luxon, B. A.; Findlay, J. B. *J. Am. Chem. Soc.* **1979**, *101*, 5869.
(15) Perrin, C. L.; Arrhenius, G. M. L. *J. Am. Chem. Soc.* **1982**, *104*, 2839.
(16) Hosie, I.; Marshall, P. J.; Sinnott, M. L. *J. Chem. Soc., Perkin Trans. 2* **1984**, 1121.
(17) Gorenstein, D. G.; Luxon, B. A.; Findlay, J. B.; Momii, R, *J. Am. Chem. Soc.* **1977**, *99*, 4170.
(18) Gorenstein, D. G.; Findlay, J. B.; Luxon, B. A.; Kar, D. *J. Am. Chem. Soc.* **1977**, *99*, 3473.
(19) Gorenstein, D. G.; Luxon, B. A.; Findlay, J. B.; *J. Am. Chem. Soc.* **1977**, *99*, 8048.

(20) Gorenstein, D. G.; Luxon, B. A.; Goldfield, E. *J. Am. Chem. Soc.* **1980**, *102*, 1757.
(21) Gorenstein, D. G.; Rowell, R.; Taira, K. In ACS Symposium, International Conference on Phosphorus Chemistry, 1981.
(22) Cieplak, A. S. *J. Am. Chem. Soc.* **1981**, *103*, 4540.
(23) Taira, K.; Gorenstein, D. G., to be submitted for publication in *Tetrahedron*.
(24) (a) Wolfe, S.; Rauk, A.; Tel, L. M.; Csizmadia, I. G. *J. Chem. Soc. B* **1971**, 136. (b) Chase, M. *White Rabbit*; Harvey Dramaticists Play Services: New York, 1944; copyright 1943.
(25) Edward, J. T. *Chem. Ind.* **1955**, 1102.
(26) Lemieux, R. U.; Koto, S. *Tetrahedron* **1974**, *30*, 1933.
(27) Lemieux, R. U.; Chu, N. *J. Am. Chem. Soc.* **1958**, *133*, 31N.
(28) Eliel, E. L.; Giza, C. A. *J. Org. Chem.* **1968**, *33*, 3754.
(29) Pierson, G. O.; Runquist, O. A. *J. Org. Chem.* **1978**, *43*, 4266.
(30) Stoddart, J. F. *Stereochemistry of Carbohydrates*; Wiley-Interscience: New York, 1971; p 72.
(31) Hutchins, R. O.; Kopp, L. D.; Eliel, E. L. *J. Am. Chem. Soc.* **1968**, *90*, 7174.
(32) Eliel, E. L. *Sven. Kem. Tidskr.* **1969**, *81*, 22.
(33) Beaulieu, N.; Dickinson, R. A.; Deslongchamps, P. *Can. J. Chem.* **1980**, *80*, 2531.
(34) Descotes, G.; Lissac, M.; Delmau, J.; Duplan, J. *C. R. Hebd. Seances Acad. Sci., Ser. C* **1968**, *267*, 1240.
(35) Hall, L. D.; Malcolm, R. B. *Can. J. Chem.* **1972**, *50*, 2092.
(36) Gorenstein, D. G.; Rowell, R. *J. Am. Chem. Soc.* **1979**, *101*, 4925–4928.
(37) Gorenstein, D. G.; Rowell, R. Findlay, J. *J. Am. Chem. Soc.* **1980**, *102*, 5077–5081.
(38) Maryanoff, B. E.; Hutchins, R. O.; Maryanoff, C. A. *Top. Stereochem.* **1979**, *11*, 187–326.
(39) Mosbo, J. A. *Org. Magn. Reson.* **1978**, *6*, 281.
(40) Bajwa, G. S.; Bentrude, W. G.; Pantaleo, N. S.; Newton, M. G.; Hargin, J. H. *J. Am. Chem. Soc.* **1979**, *101*, 1602.
(41) Hutchins, R. O.; Maryanoff, B. E.; Castillo, M. J.; Hargrave, K. D.; McPhail, A. T. *J. Am. Chem. Soc.* **1979**, *101*, 1600–1602.
(42) Gorenstein, D. G.; Kar, D. *J. Am. Chem. Soc.* **1977**, *99*, 672–677.
(43) Gorenstein, D. G.; Luxon, B. A.; Findlay, J. B. *Biochemistry* **1979**, *18*, 3796–3804.
(44) Gorenstein, D. G.; Findlay, J. B.; Momii, R. K.; Luxon, B. A.; Kar, D. *Biochemistry* **1976**, *15*, 3796–3803.
(45) Gorenstein, D. G.; In ^{31}P NMR: *Principles and Applications*; Gorenstein, D. G., Ed.; Academic: New York, 1984; Chapter 1.
(46) Gorenstein, D. G.; Luxon, B. A.; Findlay, J. B. *Biochim. Biophys. Acta* **1977**, *475*, 184–190.
(47) Mosbo, J. A.; Verkade, J. G. *J. Am. Chem. Soc.* **1972**, *94*, 8224–8225.
(48) Bentrude, W. G.; Tan, H. W. *J. Am. Chem. Soc.* **1973**, *95*, 4666.
(49) Stec, W. J.; Okruszek, A. *J. Chem. Soc., Perkin Trans. 1* **1975**, 1928.
(50) Kinas, R.; Stec, W. J.; Kruger, C. *Phosphorus Sulfur* **1978**, *4*, 294.
(51) Majoral, J. P.; Pujol, R.; Navech, J. *Bull. Soc. Chim. Fr.* **1972**, 606.
(52) Roca, C.; Kraemer, R.; Navech, J.; Brault, J. F. *Org. Magn. Reson.* **1976**, *8*, 407.
(53) Cooper, D. B.; Inch, T. D.; Lewis, G. J. *J. Chem. Soc., Perkin Trans. 1* **1974**, 1043.
(54) Harrison, J. M.; Inch, T. D.; Lewis, G. J. *J. Chem. Soc., Perkin Trans. 1* **1975**, 1892.
(55) Tsuboi, M.; Takahashi, S.; Kyoguku, Y.; Hayatsu, H.; Ukita, T.; Kainosho, M. *Science (Washington, D.C.)* **1969**, *166*, 1504.
(56) Hall, L. D.; Malcolm, R. B. *Can. J. Chem.* **1972**, *50*, 2102.
(57) Kainosho, M.; Morofushi, T.; Nakamura, A. *Bull. Chem. Soc. Jpn.* **1969**, *42*, 845.
(58) Taira, K.; Gorenstein, D. G. *Tetrahedron*, **1984**, *40*, 3215.
(59) Epiotis, N. D.; Cherry, W. R.; Shaik, S.; Yates, R. L.; Bernard, F. *Structural Theory of Organic Chemistry*; Springer-Verlag: New York, 1977.
(60) Jones, P. G.; Kirby, A. J. *J. Am. Chem. Soc.* **1984**, *106*, 6207–6212.
(61) Oie, T.; Loew, G. H.; Burt, S. K.; Binkley, J. S.; Mac-Elroy, R. D. *J. Am. Chem. Soc.* **1982**, *104*, 6179–6174.
(62) Taira, K.; Gorenstein, D. G. *Bull. Chem. Soc. Jpn.*, in press.
(63) Bizzozero, S. A.; Zweifel, B. O. *FEBS Lett.* **1975**, *59*, 105.
(64) Bizzozero, S. A.; Dutler, H. *Bioorg. Chem.* **1981**, *10*, 46.
(65) Gorenstein, D. G.; Fanni, T.; Taira, K. *J. Org. Chem.* **1984**, *49*, 4531–4536.
(66) Taira, K.; Fanni, T.; Gorenstein, D. G. *J. Am. Chem. Soc.* **1984**, *106*, 1521.
(67) Gorenstein, D. G.; Taira, K. *J. Am. Chem. Soc.* **1982**, *104*, 6130.
(68) Feather, M. S.; Haris, J. F. *J. Org. Chem.* **1965**, *30*, 153.
(69) Chandrasekhar, S.; Kirby, A. J. *J. Chem. Soc., Chem. Commun.* **1978**, 171.
(70) Kirby, A. J. *Acc. Chem. Res.* **1984**, *17*, 305.

(71) Kirby, A. J.; Martin, R. J. *J. Chem. Soc., Perkin Trans. 2* **1983**, 1627.
(72) Kirby, A. J.; Martin, R. J. *J. Chem. Soc., Perkin Trans. 2* **1983**, 1633.
(73) Briggs, A. J.; Evans, C. M.; Glenn, R.; Kirby, A. J. *J. Chem. Soc., Perkin Trans. 2* **1983**, 1637.
(74) Farcasiu, D.; Horsley, J. *J. Am. Chem. Soc.* **1980**, *102*, 4906.
(75) Perrin, C. L.; Nuñez, O. *J. Am. Chem. Soc.* **1986**, *108*, 5997.
(76) Ahmad, M.; Bergstsrom, R. G.; Cashen, M. J.; Chiang, Y.; Kresge, A. J.; McClelland, R. A.; Powell, M. F. *J. Am. Chem. Soc.* **1979**, *101*, 2669.
(77) Caswell, M.; Schmir, G. L. *J. Am. Chem. Soc.* **1979**, *101*, 7323.
(78) Sinnott, M. *Biochem. J.* **1984**, *224*, 817–821.
(79) Capon, B.; Grieve, D. M. A. *Tetrahedron Lett.* **1982**, *23*, 4823.
(80) Astudillo, M. E. A. *Tetrahedron* **1985**, *41*, 5919.
(81) Somayaji, V.; Brown, R. S. *J. Org. Chem.* **1986**, *51*, 2676.
(82) Bennet, A. J.; Sinnott, M. L. *J. Am. Chem. Soc.* **1986**, *108*, 7287–7294.
(83) Deslongchamps, P.; Chenevert, R.; Taillefer, R. J.; Moreau, C.; Saunders, J. K. *Can. J. Chem.* **1975**, *53*, 1601.
(84) Beaulieu, N.; Deslongchamps, *Can. J. Chem.* **1980**, *58*, 875.
(85) Perrin, C. L.; Nuñez, O. *J. Am. Chem. Soc.* **1987**, *109*, 522–527.
(86) Deslongchamps, P.; Atlani, P.; Frehel, D.; Malaval, A.; Moreau, C. *Can. J. Chem.* **1974**, *52*, 3651.
(87) Kaloustian, M. K.; Khouri, F. *J. Am. Chem. Soc.* **1980**, *102*, 7579.
(88) Khouri, F. F.; Kaloustian, M. K. *J. Am. Chem. Soc.* **1986**, *108*, 6683–6695.
(89) Gensmantel, N. P.; Page, M. I. *J. Chem. Soc., Perkin Trans. 2* **1979**, 137.
(90) Anet, F. A. L.; Bourn, A. J. R. *J. Am. Chem. Soc.* **1967**, *89*, 760.
(91) Jencks, W. P. *Acc. Chem. Res.* **1976**, *42*, 4203.
(92) McClelland, R. A.; Alibhai, M. *Can. J. Chem.* **1981**, *59*, 1169.
(93) Perrin, C. L.; Nuñez, O. *J. Chem. Soc., Chem. Commun.* **1984**, 333–334.
(94) Greenhouse, J. A.; Strauss, H. L. *J. Chem. Phys.* **1969**, *50*, 124.
(95) Deslongchamps, P.; Barlet, P.; Taillefer, R. *Can. J. Chem.* **1980**, *58*, 2167.
(96) Rowell, R.; Gorenstein, D. G. *J. Am. Chem. Soc.* **1981**, *103*, 5894.
(97) Taira, K.; Fanni, T.; Gorenstein, D. G.; Vaidyanathaswamy, R.; Verkade, J. G. *J. Am. Chem. Soc.* **1986**, *108*, 6311–6314.
(98) Westheimer, F. H. *Acc. Chem. Res.* **1968**, *1*, 70.
(99) Kluger, R.; Covitz, F.; Dennis, E.; Williams, L. D.; Westheimer, F. H. *J. Am. Chem. Soc.* **1969**, *91*, 6066.
(100) Covitz, F.; Westheimer, F. H. *J. Am. Chem. Soc.* **1966**, *85*, 1773.
(101) Dennis, E. A.; Westheimer, F. H. *J. Am. Chem. Soc.* **1966**, *88*, 3432.
(102) Dennis, E. A.; Westheimer, F. H. *J. Am. Chem. Soc.* **1966**, *88*, 3431.
(103) Gerlt, J. A.; Westheimer, F. H.; Sturtevant, J. M. *J. Biol. Chem.* **1975**, *250*, 5059.
(104) Buchwald, S. L.; Pliura, D. H.; Knowles, J. R. *J. Am. Chem. Soc.* **1984**, *106*, 4916.
(105) Kluger, R.; Thatcher, G. R. *J. Org. Chem.* **1986**, *51*, 207.
(106) Kluger, R.; Thatcher, G. R. *J. Am. Chem. Soc.* **1985**, *107*, 6006.
(107) Gorenstein, D. G.; Chang, A.; Yang, J. C. *Tetrahedron*, **1987**, *43*, 469–478.
(108) Brown, D. M.; Magrath, D. I.; Todd, A. R. *J. Chem. Soc.* **1955**, *2*, 4396.
(109) Streitweiser, A.; Heathcock, C. H. *Introduction to Organic Chemistry*; Macmillan: New York, 1976.
(110) Yang, J. C.; Gorenstein, D. G. *Tetrahedron* **1987**, *43*, 479–486.
(111) Chia, Y. T.; Loew, L.; Panar, M.; Westheimer, F. H. Reference 103.
(112) Kumamoto, J.; Cox, J. R., Jr.; Westheimer, F. H. *J. Am. Chem. Soc.* **1956**, *78*, 4858.
(113) Kaiser, E. T.; Panar, M.; Westheimer, F. H. *J. Am. Chem. Soc.* **1963**, *85*, 602.
(114) Asknes, G.; Bergeson, K. *Acta Chem. Scand.* **1966**, *20*, 2508.
(115) Chang, A.; Gorenstein, D. G. *Tetrahedron*, in press.
(116) Jencks, W. P. *Adv. Enzymol.* **1975**, *43*, 219.
(117) Dunathan, H. C.; Voest, J. G. *Proc. Natl. Acad. Sci. U.S.A.* **1974**, *71*, 3888–3891.
(118) Pauling, L. *Chem. Eng. News* **1946**, *24*, 1375.
(119) Wolfenden, R. *Acc. Chem. Res.* **1972**, *5*, 10.
(120) Lienhard, G. E. *Annu. Rep. Med. Chem. Res.* **1972**, *7*, 249.
(121) Albery, W. J.; Knowles, J. R. *Biochemistry* **1976**, *15*, 563.
(122) Jardetzky, O.; Roberts, G. C. K. *NMR in Molecular Biology*; Academic: New York, 1981.
(123) Hammes, G.; Schimmel, P. R. In *The Enzymes*; Boyer, P. D., Ed.; Academic: New York, 1970; Vol. II.
(124) Polgár, L.; Halász, P. *Biochem. J.* **1982**, *207*, 1–10.

(125) Angelides, K. J.; Fink, A. L. *Biochemistry* **1979**, *18*, 2363-2369.
(126) Kraut, J. *Annu. Rev. Biochem.* **1977**, *46*, 331.
(127) Fersht, A. R. *J. Am. Chem. Soc.* **1972**, *94*, 293.
(128) Caplow, M. *J. Am. Chem. Soc.* **1969**, *91*, 3639.
(129) Chesnavich, W. J.; Bowers, M. I. *J. Am. Chem. Soc.* **1976**, *98*, 8301.
(130) Blow, D. M. *Acc. Chem. Res.* **1976**, *9*, 145.
(131) Huber, R.; Bode, W. *Acc. Chem. Res.* **1978**, *11*, 114.
(132) Bode, W.; Schwager, P. *J. Mol. Biol.* **1975**, *98*, 693.
(133) Ruhlmann, A.; Kukla, D.; Schwager, P.; Barteis, K.; Huber, R. *J. Mol. Biol.* **1973**, *77*, 417.
(134) Huber, R.; Kukla, D.; Bode, W.; Schwager, P.; Barteis, K.; Dreisenhofer, J.; Steigemann, W. *J. Mol. Biol.* **1974**, *89*, 73.
(135) James, M. N. G.; Sielecki, A. R.; Brayer, G. D.; Delbaere, L. T. J.; Bayer, C. A. *J. Mol. Biol.* **1980**, *144*, 43.
(136) Kossiakoff, A. A.; Spencer, S. A. *Biochemistry* **1981**, *20*, 6462.
(137) Birktoft, J. J.; Blow, D. M. *J. Mol. Biol.* **1972**, *68*, 187.
(138) Brayer, G. D.; Delbaere, L. J. J.; James, M. N. G. *J. Mol. Biol.* **1979**, *131*, 743.
(139) Sielecki, A. R.; Hendrickson, W. A.; Broughton, C. G.; Delbaere, L. T. J.; Brayer, G. D.; James, M. N. G. *J. Mol. Biol.* **1979**, 134.
(140) Matthews, D. A.; Alden, R. A.; Birktoft, J. J.; Freer, S. T.; Kraut, J. *J. Biol. Chem.* **1977**, *252*, 8875.
(141) Matthews, D. A.; Alden, R. A.; Birktoft, J. J.; Freer, S. T.; Kraut, J. *J. Biol. Chem.* **1975**, *250*, 7120.
(142) Mavridis, A.; Tulinsky, A.; Liebman, M. N. *Biochemistry* **1974**, *13*, 3661.
(143) Burgi, H. B.; Dunitz, J. D.; Shefter, E. *J. Am. Chem. Soc.* **1973**, *95*, 5065.
(144) Scheiner, S.; Kleier, D. A.; Lipscomb, W. N. *Proc. Natl. Acad. Sci. U.S.A.* **1975**, *72*, 2606.
(145) Scheiner, S.; Lipscomb, W. M. *Proc. Natl. Acad. Sci. U.S.A.* **1976**, *73*, 432.
(146) Umeyama, H.; Imamura, A.; Nagata, C.; Hanano, M. *J. Theor. Biol.* **1973**, *41*, 485.
(147) Dugas, H.; Penney, C. *Bioorganic Chemistry, a Chemical Approach to Enzyme Action*; Springer-Verlag: New York, 1981.
(148) Petkov, D.; Christova, E.; Stoineva, I. *Biochim. Biophys. Acta* **1978**, *527*, 131.
(149) Makinen, M. W.; Kukuyama, M. W. *J. Biol. Chem.* **1982**, *257*, 24.
(150) Kuo, L. C.; Kukuyama, J. M.; Makinen, M. W. *J. Mol. Biol.* **1983**.
(151) Chang, S. H.; Rajbhandary, V. L. *J. Biol. Chem.* **1968**, *243*, 592.
(152) Quigley, G. J.; Seeman, N. C.; Wang, A. H. J.; Suddath, F. L.; Rich, A. *Nucleic Acids Res.* **1975**, *2*, 2329.
(153) Sussman, J. L.; Kim, S. H. *Biochem. Biophys. Res. Commun.* **1976**, *68*, 89.
(154) Ladner, J. E.; Jack, A.; Robertus, J. D.; Brown, R. S.; Rhodes, D.; Clark, B. F. C.; Klug, A. *Nucleic Acids Res.* **1975**, *2*, 1629.
(155) Coulter, C. L. *J. Am. Chem. Soc.* **1973**, *95*, 570.
(156) Usher, D. A.; Richardson, D. I.; Eckstein, F. *Nature (London)* **1970**, *228*, 663.
(157) Richards, R. M.; Wyckoff, H. W. In *The Enzymes*; Boyer, P. D., Ed.; Academic: New York, 1971; Vol, IV.
(158) Yakovlev, Bocharov, A. L.; Moiseev, G. P.; Mikhailov, S. K. *Bioorg. Khim.* **1985**, *11*, 205-210.
(159) Yakovlev, G. I.; Bocharov, A. C.; Moiseyev, G. P.; Mikhaylov, S. N. *FEBS* **1985**, *179*, 217-220.
(160) Cotton, F. A.; Hazen, E. E., Jr. In *The Enzymes*; Boyer, P. D., Ed.; Academic: New York, 1971; Vol. IV.
(161) Anfinsen, C. B.; Cuatrecasas, P.; Taniuchi, H. In *The Enzymes*; Boyer, P. D., Ed.; Academic: New York, 1981; Vol. IV.
(162) Dunn, B. M.; Bello, C. D.; Anfinsen, C. B. *J. Biol. Chem.* **1973**, *248*, 4769.
(163) Cotton, F. A.; Bier, C. J.; Day, V. W.; Hazen, E. E.; Larsen, S. *Cold Spring Harbor Symp. Quant. Biol.* **1972**, *36*, 243-249.
(164) Cotton, F. A.; Hazen, E. E., Jr.; Legg, M. J. *Proc. Natl. Acad. Sci. U.S.A.* **1979**, *76*, 2551-2555.
(165) Deiters, J. A.; Calluci, J. C.; Holmes, R. R. *J. Am. Chem. Soc.* **1982**, *104*, 5457-5465.
(166) Hibler, D. W.; Gerlt, J. A. *Fed. Proc., Fed. Am. Soc.* **1987**, *45*, 1875.
(167) Serpersu, E. H.; Shortle, D.; Mildvan, A. S. *Biochemistry*, in press.
(168) Saenger W. *Principles of Nucleic Acid Structure*; Springer-Verlag: New York, 1984.
(169) Calladine, C. R. *J. Mol. Biol.* **1982**, *161*, 343-352.
(170) Dickerson, R. E. *J. Mol. Biol.* **1983**, *166*, 419-441.
(171) Dickerson, R. E.; Drew, H. R. *J. Mol. Biol.* **1981**, *149*, 761-786.
(172) Anderson, J. E.; Ptashne, M.; Harrison, S. C. *Nature (London)* **1985**, *316*, 596.
(173) McClarin, J. A.; Frederick, C. A.; Wang, B. C.; Greene, P.; Boyer, H. W.; Grable, J.; Rosenberg, J. M. *Science (Washington, D.C.)* **1986**, *234*, 1526.
(174) Richmond, T. J.; Finch, J. T.; Rushton, B.; Rhodes, D.; Klug, A. *Nature (London)* **1985**, *311*, 532.
(175) Martin, K.; Schleif, R. F. *Proc. Natl. Acad. Sci. U.S.A.* **1986**, *83*, 3654.
(176) Hochschild, A.; Ptashne, M. *Cell* **1986**, *44*, 681.
(177) Gorenstein, D. G.; Schroeder, S. A.; Miyasaki, M.; Fu, J. M.; Roongta, V.; Abuaf, P.; Chang, A.; Yang, J. C. In *Proceedings of the 2nd International Symposium on Phosphorus Chemistry Directed towards Biology*; Elsevier: Amsterdam, 1986.
(178) Klug, A.; Viswamitra, M. A.; Kennard, O.; Shakked, Z.; Steitz, T. A. *J. Mol. Biol.* **1979**, *131*, 669-680.
(179) Gorenstein, D. G. In *Jerusalem Symposium, NMR in Molecular Biology*; Pullman, B., Ed.; D. Reidel: Dordrecht 1978; Vol. 11, pp 1-15.
(180) Gorenstein, D. G. *Annu. Rev. Biophys. Bioeng.* **1981**, *10*, 355.
(181) Gorenstein, D. G. In *^{31}P NMR: Principles and Applications*; Gorenstein, D., Ed.; Academic: New York, 1984.
(182) Gorenstein, D. G. *Prog. Nucl. Magn. Reson. Spectrosc.* **1983**, *161*, 1-98.
(183) Gorenstein, D. G.; Kar, D.; Momii, R. K. *Biochem. Biophys. Res. Commun.* **1976**, *73*, 105.
(184) Prado, F. R.; Geissner-Prettre, C.; Pullman, B.; Daudey, J. P. *J. Am. Chem. Soc.* **1979**, *101*, 1737-1742.
(185) Sundaralingam, M. *Biopolymers* **1969**, *7*, 821-860.
(186) Shah, D. O.; Lai, K.; Gorenstein, D. G. *Biochemistry* **1984**, *23*, 6717-6723.
(187) Shah, D. O.; Lai, K.; Gorenstein, D. G. *J. Am. Chem. Soc.* **1984**, *106*, 4302.
(188) Schroeder, S.; Jones, C.; Fu, J.; Gorenstein, D. G. *Bull. Magn. Reson.* **1986**, *8*, 137-146.
(189) Schroeder, S.; Fu, J.; Jones, C.; Gorenstein, D. G. *Biochemistry* **1987**, *26*, 3812-3821.
(190) Petersheim, M.; Mehdi, S.; Gerlt, J. A. *J. Am. Chem. Soc.* **1984**, *106*, 439.
(191) Ott, J.; Eckstein, F. *Biochemistry* **1985**, *24*, 253.
(192) Ott, J.; Eckstein, F. *Nucleic Acids Res.* **1985**, *13*, 6317-6330.
(193) Eckstein, F.; Jovin, T. M. *Biochemistry* **1983**, *22*, 4546.
(194) Lomonossof, G. P.; Butler, P. J. G.; Klug, A. *J. Mol. Biol.* **1981**, *149*, 745-760.
(195) Drew, H. R.; Travers, A. A. *Cell* **1984**, *37*, 491-502.
(196) Scheffler, I. E.; Elson, E. L.; Baldwin, R. L. *J. Mol. Biol.* **1968**, *36*, 291-304.
(197) Viswamitra, M. A.; Kennard, O.; Shakked, Z.; Jones, D. G.; Sheldrick, G. M.; Salisbury, S.; Falvello, L. *Nature (London)* **1978**, *273*, 687-690.
(198) Shindo, H.; Simpson, R. T.; Cohen, J. S. *J. Biol. Chem.* **1979**, *254*, 8125.
(199) Ford, L. O.; Johnson, L. N.; Mechin, P. A.; Phillips, D. C.; Tjian, R. *J. Mol. Biol.* **1974**, *88*, 349.
(200) Warshel, A.; Levitt, M. *J. Mol. Biol.* **1976**, *103*, 227-249.
(201) Hosie, L.; Sinnott, M. L. *Biochem. J.* **1985**, *226*, 437-446.
(202) Chipman, D. M.; Sharon, N. *Science (Washington, D.C.)* **1969**, *165*, 454.
(203) Kelly, J. A.; Sielecki, A. R.; Sykes, B. D.; Philips, D. C. *Nature (London)* **1979**, *282*, 875.
(204) Platt, S. L.; Baldo, J. H.; Boekelheide, K.; Weiss, G.; Sykes, B. D. *Can. J. Biochem.* **1978**, *56*, 624.
(205) Schindler, M.; Aesaf, Y.; Sharon, N.; Chipman *Biochemistry* **1977**, *16*, 423.
(206) Post, C. B.; Karplus, M. *J. Am. Chem. Soc.* **1986**, *108*, 1317-1319.
(207) Pincus, M. R.; Scheraga, H. A. *Macromolecules* **1979**, *12*, 633.
(208) Post, C. B.; Brooks, B. R.; Karplus, M.; Dobson, C. M.; Artymiuk, P. J.; Cheetham, J. C.; Philips, D. C. *J. Mol. Biol.* **1986**, *190*, 455-479.
(209) Benner, S. A. *Experientia* **1983**, *38*, 633-637.
(210) Nambiar, K. P.; Stauffer, D. M.; Kolodziej, P. A.; Benner, S. A. *J. Am. Chem. Soc.* **1983**, *105*, 5886-5890.
(211) Benner, S. A.; Nambiar, K. P.; Chambers, G. K. *J. Am. Chem. Soc.* **1985**, *107*, 5513-5517.
(212) Fisher, H. F.; Conn, E. E.; Vennesland, B.; Westheimer, F. H. *J. Biol. Chem.* **1953**, *202*, 687-697.
(213) Oppenheimer, N. J. *J. Am. Chem. Soc.* **1984**, *106*, 3032-3033.
(214) Rob, F.; Van Ramesdonk, H. J.; Van Gerresheim, W.; Bosma, P.; Scheele, J. J.; Verhoeven, J. W. *J. Am. Chem. Soc.* **1984**, *106*, 3826-3832.
(215) You, K. S. *CRC Crit. Rev. Biochem.* **1984**, *17*, 313-451.
(216) Sklenář, V.; Miyashiro, H.; Zon, G.; Miles, H. T.; Bax, A. *FEBS Lett.* **1986**, *208*, 94-98.
(217) Jones, R. L.; Wilson, W. D. *J. Am. Chem. Soc.* **1980**, *102*, 7776-7778.